Electronic Thesis and Dissertation Repository

8-10-2016 12:00 AM

Fractional Charge Methods for Correcting Approximate Kohn-Sham Potentials

Darya N. Komsa, *The University of Western Ontario*

Supervisor: Viktor N. Staroverov, *The University of Western Ontario*
A thesis submitted in partial fulfillment of the requirements for the Master of Science degree in Chemistry
© Darya N. Komsa 2016

Follow this and additional works at: https://ir.lib.uwo.ca/etd

Part of the Atomic, Molecular and Optical Physics Commons, and the Physical Chemistry Commons

Recommended Citation

Abstract

The Kohn-Sham density functional theory, a widely used approach for calculating electronic properties of atoms and molecules, relies on approximating the exchange-correlation energy functional or the corresponding potential, v_{XC}. Whether the exchange-correlation potential is modeled directly or derived from its parent energy functional, its behavior as a function of position in an atom or a molecule can be used to detect and correct deficiencies of the parent density functional approximation. The too-fast decay of v_{XC} derived from common density functionals is a major problem, because it causes inaccurate Rydberg excitation energies and erroneous fractional charges in dissociating molecules. An efficient method to correct the shape of the exchange-correlation potential in the asymptotic regions was proposed by Gaiduk *et al.* [A. P. Gaiduk, D. S. Firaha, and V. N. Staroverov, Phys. Rev. Lett. **108**, 253005 (2012)]. In that method, the exchange-correlation potential of an auxiliary system with a fractionally occupied frontier orbital is used to construct a model potential for the neutral system of interest. In this thesis, we investigate a method to eliminate unphysical partial charges on atoms in dissociating polar molecules via the use of the fractional occupation technique. The method proves successful not only for enforcing correct integer charges in the dissociation limit, but also for predicting how atomic charges change at intermediate interatomic separations. We also test the hypothesis that a fractionally charged system with an integral number of electrons but fractional *nuclear* charge may be used to correct the exchange-correlation potential in order to obtain more accurate Rydberg excitation energies. Our findings show that, although the model potentials generated in this way give rise to some improvements, the optimal nuclear charge to be added depends on the system. In contrast, the advantage of the method of fractional orbital occupations is that the parameter required to correct excitation energies is system-independent.

Keywords: quantum chemistry, density functional theory, exchange-correlation potential, fractionally charged systems, partial charge, self-interaction error.

Co-Authorship Statement

Chapter 2 is based on the manuscript in preparation "Elimination of spurious fractional charges in dissociating molecules by correcting the shape of approximate Kohn-Sham potentials" by Darya N. Komsa and Viktor N. Staroverov. Darya N. Komsa carried out all the calculations and wrote its text. The code for the calculations on systems with fractional numbers of electrons was written by Dr. Alex Gaiduk. Chapter 3 is based on the manuscript in preparation "Excitation energies from Kohn-Sham potentials corrected via addition of fractional nuclear charge" by Darya N. Komsa and Viktor N. Staroverov. Darya N. Komsa performed the calculations and wrote its text.

Acknowledgments

Since the beginning of my undergraduate studies, it was my dream to come to Canada to pursue a graduate degree. I am delighted that this dream has come true and I would like to take this opportunity to thank the people who have helped me progress to my M.Sc.

First of all, I am incredibly grateful to my supervisor, Professor Viktor N. Staroverov, for his support and willingness to help at any time. I admire his passion for science and his aspiration for perfection. I particularly appreciate Viktor's showing me that enthusiasm is a key to success in any field.

I am very thankful to our former group member Dr. Alex Gaiduk who wrote the code which I used in many calculations. He was also the one who encouraged me to join the group in the summer of 2013, and I am immensely grateful to him for doing this. I would like to thank my colleagues, Dr. Amin Torabi, Zitong Wang, Dzmitry Shakhno, Rayner Mendes, Dr. Rogelio Cuevas-Saavedra, Slava Kohut, Hanqing Zhao, Angela Murcia Rios, Dr. Egor Ospadov, and Victor Hugo Chávez, for joyful conversations and maintaining a warm atmosphere. A special thank you goes to Rogelio for the evenings at the grad club, to Slava for being an amazing roommate, to Egor for proofreading parts of this work.

I also want to thank my dearest friend Tanya for endless support, motivation, and patience. She was always there whenever I needed someone to listen. Lastly, my deepest gratitude goes to my family, my sister Tanya and my parents. I owe them everything I achieved.

Прысьвячаецца маім бацькам і сястрычцы Танечцы

Contents

List of Abbreviations

B3LYP	—	Becke-Lee-Yang-Parr hybrid
BLYP	—	Becke-Lee-Yang-Parr
C	—	correlation
DFA	—	density functional approximation
DFT	—	density functional theory
EOM-CCSD	—	equation of motion coupled cluster singles and doubles
EXX	—	exact exchange
FMO	—	frontier molecular orbital
GGA	—	generalized gradient approximation
H	—	Hartree
HF	—	Hartree-Fock
HOMO	—	highest occupied molecular orbital
HXC	—	Hartree-exchange-correlation
LC-ωPBE	—	long-range corrected Perdew-Burke-Ernzerhof
LDA	—	local density approximation
LUMO	—	lowest unoccupied molecular orbital
M06	—	Minnesota 06
MAE	—	mean absolute error
NPA	—	natural population analysis
PBE	—	Perdew-Burke-Ernzerhof
PBE0	—	Perdew-Burke-Ernzerhof hybrid
SCF	—	self-consistent field
SIC	—	self-interaction correction
SIE	—	self-interaction error
TDDFT	—	time-dependent density functional theory
TPSS	—	Tao-Perdew-Staroverov-Scuseria

List of Symbols

a_0	—	atomic unit of length ($1\,\text{bohr} = 0.529177\,\text{Å}$)
A	—	electron affinity
E	—	total energy
E_X	—	exchange energy
E_C	—	correlation energy
E_{XC}	—	exchange-correlation energy
E_h	—	atomic unit of energy ($1\,\text{hartree} = 2625.50\,\text{kJ}\,\text{mol}^{-1} = 27.2114\,\text{eV}$)
ε	—	molecular orbital eigenvalue
f	—	general energy density
ϕ_i	—	Kohn-Sham orbitals
I	—	ionization potential
J	—	Coulomb repulsion energy
M	—	number of nuclei
N	—	number of electrons
q	—	atomic charge
$\mathbf{r}$	—	position vector
$\mathbf{R}$	—	position vector of a nucleus
R_c	—	critical radius
R_e	—	equilibrium internuclear separation
ρ	—	electron density
v	—	external potential
v_s	—	Kohn-Sham potential
v_H	—	Hartree potential
v_{HXC}	—	Hartree-exchange-correlation potential
v_{XC}	—	exchange-correlation potential
V	—	energy of electrons due to external field
V_{ee}	—	energy of electron-electron interaction
ω	—	highest occupied molecular orbital depopulation (if negative) or lowest unoccupied molecular orbital population (if positive)
Z	—	nuclear charge
ζ	—	fraction of positive charge added to the nuclei

Chapter 1

Introduction

1.1 Density functional theory

The description of electronic structure of molecules in the ground state relies on solving the non-relativistic time-independent Schrödinger equation,

$$\hat{H}\Psi(\mathbf{x}_1, \mathbf{x}_2, ..., \mathbf{x}_N) = E\Psi(\mathbf{x}_1, \mathbf{x}_2, ..., \mathbf{x}_N), \tag{1.1}$$

where $\hat{H}$ is the electronic Hamiltonian operator, E is the total ground-state energy, and $\Psi(\mathbf{x}_1, \mathbf{x}_2, ..., \mathbf{x}_N)$ is the ground-state electronic wavefunction, which depends on the positions and spins $\mathbf{x}_i \equiv \{\mathbf{r}_i, \sigma_i\}$ of all of the N electrons in the system. The Hamiltonian of an N-electron system can be written as the sum of the operators for the kinetic energy of the electrons, $\hat{T}$, the energy of interaction of the electrons with the external potential $v(\mathbf{r})$ (typically due to the nuclei), $\hat{V}$, and the energy of the electron-electron interaction, $\hat{V}_{\text{ee}}$ [1]:

$$\hat{H} = \hat{T} + \hat{V} + \hat{V}_{\text{ee}} = -\frac{1}{2}\sum_{i=1}^{N}\nabla_i^2 + \sum_{i=1}^{N}v(\mathbf{r}_i) + \sum_{i<j}^{N}\frac{1}{|\mathbf{r}_i - \mathbf{r}_j|}. \tag{1.2}$$

Here and below, we employ the system of atomic units to present equations in a compact form.

Analytical solutions of the Schrödinger equation are only available for a limited number of one- and two-electron systems, such as the hydrogen atom and the hydrogen molecular ion. For a many-electron system, the Schrödinger equation can be solved only approximately. The approximate wavefunction has to satisfy the fundamental property of the exact Ψ, which is its antisymmetry with respect to an interchange of the coordinates of any two electrons: $\Psi(\mathbf{x}_2, \mathbf{x}_1, ..., \mathbf{x}_N) = -\Psi(\mathbf{x}_1, \mathbf{x}_2, ..., \mathbf{x}_N)$. The simplest solution

is to use a Slater determinant, that is, an antisymmetrized product of N orbitals, ϕ_i:

$$\Phi(\mathbf{x}_1, \mathbf{x}_2, ..., \mathbf{x}_N) = (N!)^{-1/2} \begin{vmatrix} \phi_1(\mathbf{x}_1) & \phi_2(\mathbf{x}_1) & \cdots & \phi_N(\mathbf{x}_1) \\ \phi_1(\mathbf{x}_2) & \phi_2(\mathbf{x}_2) & \cdots & \phi_N(\mathbf{x}_2) \\ \vdots & \vdots & & \vdots \\ \phi_1(\mathbf{x}_N) & \phi_2(\mathbf{x}_N) & \cdots & \phi_N(\mathbf{x}_N) \end{vmatrix}, \tag{1.3}$$

where $(N!)^{-1/2}$ is a normalization factor. In practical calculations, the spatial parts of the orbitals are linear expansions in a set of predefined basis functions. The form of the approximate Ψ of Eq. 1.3 is used in the Hartree-Fock (HF) theory [2, 3]. More sophisticated wavefunction-based methods [4–6] expand Ψ as a sum of Slater determinants.

The most computationally expensive step of a HF calculation is the calculation of $\mathcal{O}(N^4)$ two-center two-electron integrals. In highly accurate wavefunction-based methods, the approximate wavefunction becomes more complex, and evaluation of a larger number of two-electron integrals is required. Consequently, these methods scale less favourably, up to $\mathcal{O}(N^7)$ [7] and even $\mathcal{O}(N!)$ [1], which makes their application to large systems, such as biomolecules, impossible.

An alternative became available in 1964, when Hohenberg and Kohn proved [8] that the energy and electronic properties of atoms and molecules in the ground state are uniquely defined by the electron density $\rho(\mathbf{r})$. This statement, the first Hohenberg-Kohn theorem, is the foundation of density functional theory (DFT), one of the most widely used electronic structure calculation methods. In a DFT calculation, the evaluation of two-center two-electron integrals is usually not necessary, therefore, DFT outperforms wavefunction-based methods in terms of computational scaling with system size, and enables calculations on proteins and periodic systems with thousands of atoms [9].

For a molecule with N electrons, the electron density $\rho(\mathbf{r})$ is defined as the following integral over the spin coordinates of all electrons and over all but one of the spatial coordinates:

$$\rho(\mathbf{r}) = N \int \cdots \int |\Psi(\mathbf{x}_1, \mathbf{x}_2, ..., \mathbf{x}_N)|^2 d\sigma_1 d\mathbf{x}_2 \ldots d\mathbf{x}_N. \tag{1.4}$$

The electron density is a probability density function, which, when multiplied by an infinitely small volume element $d\mathbf{r}$ near the point $\mathbf{r}$, gives the probability of finding any of the N electrons with arbitrary spin within $d\mathbf{r}$ while the other $(N-1)$ electrons have arbitrary positions. Time-independent DFT only deals with ground-state densities, hence, from now on, the terms "electron density" or simply "density" will refer to the ground-state electron density of the system.

In DFT, there exists a rule that assigns the value of the total ground-state energy

E to the electron density $\rho(\mathbf{r})$, which is itself a function of $\mathbf{r}$. The mathematical term for such a rule is a functional. A functional can be regarded as a function of a function. Thus, one can say that the ground-state energy can be expressed as a functional of the electron density (hence the name DFT):

$$E = E[\rho]. \tag{1.5}$$

Furthermore, according to the second Hohenberg-Kohn theorem [8], the energy density functional is variational. That is, for a trial density ρ, which is not the ground-state density, it gives an energy above the ground-state energy E_0:

$$E[\rho] \geq E_0. \tag{1.6}$$

This holds for any density that can be produced by some external potential (a v-representable density) [10]. The variational principle provides a way of finding the ground-state density by minimizing the total energy [11, 12].

If one knew the exact form of the energy functional $E[\rho]$, then obtaining the exact ground-state ρ and E would not require solving the Schrödinger equation. Unfortunately, $E[\rho]$ is extremely complicated, and its exact form is unknown, so that in practice one has to resort to density functional approximations (DFAs).

1.1.1 Kohn-Sham approach

In the same way as with the Hamiltonian, one can partition the energy functional $E[\rho]$ into several terms: the kinetic energy functional, $T[\rho]$, the energy due to the external electrostatic potential, $V[\rho]$, and the energy of electron-electron interactions, $V_{\mathrm{ee}}[\rho]$:

$$E[\rho] = T[\rho] + V[\rho] + V_{\mathrm{ee}}[\rho]. \tag{1.7}$$

The kinetic energy and the electron-electron interaction energy do not have explicit forms in terms of the density. These two terms constitute a large part of the total energy. Thus, devising a functional that would approximate the entire $T[\rho]$ and $V_{\mathrm{ee}}[\rho]$ is undesirable. This obstacle is overcome in the Kohn-Sham method.

In the Kohn-Sham approach [13], one starts by introducing a fictitious system, in which electrons do not interact with each other. For such a system, the electron-electron interaction term $V_{\mathrm{ee}}[\rho]$ in Eq. 1.7 disappears, and the energy functional becomes

$$E_s[\rho] = T_s[\rho] + V_s[\rho], \tag{1.8}$$

where the symbol s denotes that the system is non-interacting. Thus, $T_s[\rho]$ is the kinetic energy of non-interacting electrons, it can be calculated exactly, and $V_s[\rho] = \int v_s(\mathbf{r})\rho(\mathbf{r})d\mathbf{r}$ is the energy due to the external potential. The energy of the non-interacting system, E_s, corresponds to such a Hamiltonian of Eq. 1.2, in which there is no electron-electron interaction term. One can map this fictitious system to the real system of interest by noting that it is possible to adjust the external potential, $v_s(\mathbf{r})$, in such a way that this potential will give rise to the electron density equal to the ground-state density of the system of interest. This leads to the following energy functional of the real interacting system:

$$E[\rho] = T_s[\rho] + V[\rho] + J[\rho] + E_{\text{XC}}[\rho], \tag{1.9}$$

where $T_s[\rho]$ is the part of kinetic energy of electrons, which only accounts for their uncorrelated motion, $J[\rho]$ is the Coulomb repulsion energy of electrons:

$$J[\rho] = \frac{1}{2} \int \int \frac{\rho(\mathbf{r})\rho(\mathbf{r}')}{|\mathbf{r} - \mathbf{r}'|} d\mathbf{r}d\mathbf{r}'. \tag{1.10}$$

In the absence of external electric fields, $V[\rho]$ comes only from the electrostatic attraction of the electrons to the nuclei and can be written as

$$V[\rho] = -\sum_{A=1}^{M} \int \frac{Z_A}{|\mathbf{r} - \mathbf{R}_A|} \rho(\mathbf{r})d\mathbf{r}, \tag{1.11}$$

where Z_A is the charge of the A-th nucleus, $\mathbf{R}_A$ is its position, and M is the total number of nuclei.

The last term in Eq. 1.9, $E_{\text{XC}}[\rho]$, is called the *exchange-correlation energy functional*. It takes care of the electron-electron interactions that are not accounted for by other terms. The exchange energy, E_{X}, is associated with the antisymmetry of an electronic wavefunction with respect to the exchange of the coordinates of two electrons. The exact exchange energy (EXX) in DFT is given by the same expression as the exchange energy in the HF theory:

$$E_{\text{X}}^{\text{exact}} = -\frac{1}{2} \sum_{i,j}^{N} \int \int \frac{\phi_i^*(\mathbf{r})\phi_j^*(\mathbf{r}')\phi_j(\mathbf{r})\phi_i(\mathbf{r}')}{|\mathbf{r} - \mathbf{r}'|} d\mathbf{r}d\mathbf{r}', \tag{1.12}$$

but instead of the HF orbitals, the Kohn-Sham orbitals, ϕ_i, are used. The correlation energy can then be obtained as the following difference:

$$E_{\text{C}} = E_{\text{XC}} - E_{\text{X}}^{\text{exact}}. \tag{1.13}$$

However, in practice one usually uses approximate expressions for E_X, and the division of the exchange-correlation energy into the exchange and correlation terms is arbitrary.

The key benefit of the mapping between the real system and the non-interacting one is that it allows one to transform the formidable problem of solving the many-body Schrödinger equation (Eq. 1.1) into a manageable task of solving N one-electron Kohn-Sham equations of the form

$$\left[-\frac{1}{2}\nabla^2 + v_{\text{eff}}([\rho]; \mathbf{r}) \right] \phi_i(\mathbf{r}) = \varepsilon_i \phi_i(\mathbf{r}), \tag{1.14}$$

where $\phi_i(\mathbf{r})$ are Kohn-Sham orbitals, and ε_i are their eigenvalues. The effective Kohn-Sham potential v_{eff} is the functional derivative of $E[\rho] - T_s[\rho]$ with respect to the electron density.

The functional derivative of a functional $F[f]$ can be defined through the variation δF of this functional, which results from variation of f by $\delta f = \epsilon\eta$, where ϵ is an infinitesimal number and η is an arbitrary integrable function. One can use a Taylor expansion around $\epsilon = 0$ for δF to obtain

$$\delta F = F[f + \epsilon\eta] - F[f] = \left. \frac{dF[f + \epsilon\eta]}{d\epsilon} \right|_{\epsilon=0} \epsilon + \frac{1}{2} \left. \frac{d^2 F[f + \epsilon\eta]}{d\epsilon^2} \right|_{\epsilon=0} \epsilon^2 + \ldots \tag{1.15}$$

By keeping only the first-order term in the expansion, one arrives at

$$\lim_{\epsilon\to 0} \frac{F[f + \epsilon\eta] - F[f]}{\epsilon} = \left. \frac{dF[f + \epsilon\eta]}{d\epsilon} \right|_{\epsilon=0}. \tag{1.16}$$

Then the functional derivative $v([f]; \mathbf{r}) = \delta F / \delta f(\mathbf{r})$, where f is a function of $\mathbf{r}$, is defined as

$$\int v([f]; \mathbf{r})\eta(\mathbf{r})d\mathbf{r} = \int \frac{\delta F}{\delta f(\mathbf{r})}\eta(\mathbf{r})d\mathbf{r} = \left. \frac{dF[f + \epsilon\eta]}{d\epsilon} \right|_{\epsilon=0}. \tag{1.17}$$

For a particular case when $f = \rho$, $F[f] = E[\rho] - T_s[\rho] = V[\rho] + J[\rho] + E_{\text{XC}}[\rho]$, and $\eta = \delta\rho$, one has

$$v_{\text{eff}}([\rho]; \mathbf{r}) \equiv \frac{\delta(V[\rho] + J[\rho] + E_{\text{XC}}[\rho])}{\delta\rho(\mathbf{r})}. \tag{1.18}$$

The effective potential can be written as the sum of the functional derivatives of $V[\rho]$, $J[\rho]$, and $V_{\text{XC}}[\rho]$. These are the external potential $v(\mathbf{r})$

$$v(\mathbf{r}) = \frac{\delta V[\rho]}{\delta\rho(\mathbf{r})} = -\sum_{A=1}^{M} \frac{Z_A}{|\mathbf{r} - \mathbf{R}_A|}, \tag{1.19}$$

the Hartree potential $v_\mathrm{H}(\mathbf{r})$

$$v_\mathrm{H}([\rho];\mathbf{r}) = \frac{\delta J[\rho]}{\delta\rho(\mathbf{r})} = \int \frac{\rho(\mathbf{r}')}{|\mathbf{r}-\mathbf{r}'|}d\mathbf{r}', \tag{1.20}$$

and the exchange-correlation potential $v_\mathrm{XC}(\mathbf{r})$

$$v_\mathrm{XC}([\rho];\mathbf{r}) = \frac{\delta E_\mathrm{XC}[\rho]}{\delta\rho(\mathbf{r})}. \tag{1.21}$$

The sum of v_H and v_XC is often referred to as the Hartree-exchange-correlation potential, v_HXC. The Hartree-exchange-correlation potential accounts for all electron-electron interactions in the system.

After inserting the available expressions for the potentials from Eqs. 1.19 and 1.20, the Kohn-Sham equations (Eq. 1.14) can be rewritten as

$$\left[-\frac{1}{2}\nabla^2 + v(\mathbf{r}) + v_\mathrm{H}([\rho];\mathbf{r}) + v_\mathrm{XC}([\rho];\mathbf{r})\right]\phi_i(\mathbf{r}) = \varepsilon_i\phi_i(\mathbf{r}). \tag{1.22}$$

Similarly to the exchange-correlation functional, the exchange-correlation potential is the only term in Eq. 1.22 that does not have an exact expression relating it to $\rho(\mathbf{r})$. If a DFA is designed by approximating the exchange-correlation energy functional $E_\mathrm{XC}[\rho]$ (this is the most common route), then the exchange-correlation potential, v_XC, can be obtained via Eq. 1.21 using techniques of functional differentiation. An alternative is to devise an approximate form for v_XC directly. Such exchange-correlation potentials are called model potentials.

With an approximate form for either $E_\mathrm{XC}[\rho]$ or v_XC at hand, one can proceed to solve the Kohn-Sham equations (Eq. 1.22). The objective is to find the Kohn-Sham orbitals $\phi_i(\mathbf{r})$, since the electron density $\rho(\mathbf{r})$ can be calculated as the sum of the squares of the Kohn-Sham orbitals:

$$\rho(\mathbf{r}) = \sum_{i=1}^{N} |\phi_i(\mathbf{r})|^2. \tag{1.23}$$

However, Eq. 1.22 contains terms that depend on the yet unknown density ($v_\mathrm{HXC} = v_\mathrm{H} + v_\mathrm{XC}$). Therefore, the Kohn-Sham equations have to be solved self-consistently. In a self-consistent procedure one starts with a guess for the Kohn-Sham orbitals, evaluates $v_\mathrm{HXC}([\rho];\mathbf{r})$, and finds the new Kohn-Sham orbitals by solving Eq. 1.22. The new orbitals are used to construct the new $v_\mathrm{HXC}([\rho];\mathbf{r})$, and the above steps are repeated until the orbitals do not change any more.

It should be noted that the Kohn-Sham method is formally exact. That is, no ap-

proximations are introduced during the derivation of the Kohn-Sham equations, and, if the exact E_{XC} were used, one would obtain the exact ground-state density and energy. Unfortunately, the exact $E_{\text{XC}}[\rho]$ and v_{XC} are out of reach. Some features of the exact exchange-correlation energy functional and potential are known, as well as their form for certain special cases, such as hydrogen-like atoms. These provide guidance for the construction of new density functional approximations. However, there is no systematic way of improving density functionals. Along with the approximations that satisfy as many exact constraints as possible and can be considered non-empirical, there are ones that use fitting and violate the constraints while still showing excellent performance.

1.2 The ladder of density functionals

Local density approximation

The simplest approach used to model electrons in a real system is to treat them as a uniform electron gas, where electrons move in the field of a constant positive background charge and the electron density is constant everywhere. This simplification allows one to derive an energy functional known as the *local density approximation* (LDA) [13]:

$$E_{\text{XC}}^{\text{LDA}}[\rho] = \int f_{\text{XC}}^{\text{LDA}}(\rho(\mathbf{r}))d\mathbf{r}, \tag{1.24}$$

where the exchange-correlation energy density f_{XC} is a function of the density only. LDA is local in the sense that the energy density at a particular point $\mathbf{r}$ in the system depends only on ρ at that particular point, and is independent of its surroundings. The exchange-correlation energy density can be split into the exchange and correlation parts, with the exchange term, f_{X}, being the dominant contributor. The exact f_{X} has a simple analytic expression [14, 15]:

$$f_{\text{X}}^{\text{LDA}}(\rho(\mathbf{r})) = -\frac{3}{4}\left(\frac{3}{\pi}\right)^{1/3}\rho^{1/3}(\mathbf{r}). \tag{1.25}$$

The correlation term, $f_{\text{C}}^{\text{LDA}}$, is not available in exact form, but the existing analytical expressions are very accurate. Of course, LDA is an exact method only for the uniform electron gas. Taking into account that the electron density in atoms and molecules is highly non-uniform, one would expect LDA to provide poor description of real systems. Surprisingly, the results are not very bad: for some properties, such as molecular geometries, LDA even outperforms the HF approximation [9].

Generalized gradient approximations

Although, in principle, the density should be the only ingredient necessary to determine the exchange-correlation energy, it is more practical to construct flexible exchange-correlation functionals in approximate DFT by adding more density-dependent terms. In order to take care of the rapid change of densities in atoms and molecules, an exchange-correlation functional should have a nonlocal ingredient—the density gradient, $\nabla\rho$. The functionals that depend not only on ρ, but also on $\nabla\rho$, are called *generalized gradient approximations* (GGA) and can be generally written as

$$E_{\mathrm{XC}}^{\mathrm{GGA}}[\rho] = \int f_{\mathrm{XC}}^{\mathrm{GGA}}(\rho(\mathbf{r}), \nabla\rho(\mathbf{r}))d\mathbf{r}. \tag{1.26}$$

The development of GGAs brought density functional theory to a whole new level since reasonably accurate calculations (previously available only for solid-state materials with LDA) became possible for molecules.

Meta-generalized gradient approximations

Further improvements to $E_{\mathrm{XC}}[\rho]$ can be achieved by introducing dependence on even more terms. It seemed natural to include the Laplacian of the density and higher-order terms, but such functionals were found to suffer from numerical instabilities [16]. Another option proven to be successful is to utilize the kinetic energy density $\tau(\mathbf{r})$. The kinetic energy density integrates to the non-interacting kinetic energy T_s (hence the name). It depends on ρ implicitly through the orbitals ϕ_i:

$$\tau(\mathbf{r}) = \frac{1}{2}\sum_{i=1}^{N}|\nabla\phi_i(\mathbf{r})|^2. \tag{1.27}$$

The functionals that depend on the kinetic energy density, in addition to the density gradient and the density itself, are known as *meta-generalized gradient approximations*. The general form of a meta-GGA is

$$E_{\mathrm{XC}}^{\text{meta-GGA}}[\rho] = \int f_{\mathrm{XC}}^{\text{meta-GGA}}(\rho(\mathbf{r}), \nabla\rho(\mathbf{r}), \tau(\mathbf{r}))d\mathbf{r}. \tag{1.28}$$

The three types of density functionals discussed, LDA, GGA, and meta-GGA, are often collectively referred to as *semi-local* functionals. The term semi-local means that the ingredients of these functionals, ρ, $\nabla\rho$, and τ, at a given point $\mathbf{r}$ depend on the density or orbitals only in the vicinity of $\mathbf{r}$.

Hybrid functionals

Nowadays, the most popular density functionals are *hybrid functionals*. These are constructed by combining GGAs or meta-GGAs with the exact exchange. First, let us explain what is meant by the exact exchange.

Recall that the exchange-correlation energy functional can be split into the exchange and the correlation parts, E_X and E_C, the exchange contribution is significantly larger than the correlation. The exchange energy can be calculated exactly. The expression for the exact exchange (EXX) is borrowed from the HF theory,

$$E_X^{\text{exact}} = -\frac{1}{2} \sum_{i,j}^{N} \int \int \frac{\phi_i^*(\mathbf{r})\phi_j^*(\mathbf{r}')\phi_j(\mathbf{r})\phi_i(\mathbf{r}')}{|\mathbf{r} - \mathbf{r}'|} d\mathbf{r} d\mathbf{r}', \tag{1.29}$$

with the only difference that the orbitals used to evaluate EXX are not the Hartree-Fock, but the Kohn-Sham orbitals.

It seems rational to use the exact expression for the exchange part and approximate only the correlation part, instead of approximating the whole E_{XC}. Indeed, the resulting functional has some appealing features that will be discussed later. Nonetheless, its accuracy is unsatisfactory in general applications. For example, the error in atomization energies is about six times higher than that of GGAs [9]. Since the exact exchange part is non-local while the approximate correlation is local, it appears that their combination lacks important cancellation of errors that occurs in a fully approximate E_{XC}. Besides, the integration in Eq. 1.29 is a computationally demanding task [17].

Combining EXX with approximate exchange makes it possible to have the cancellation of errors occur, just as in semi-local functionals, but with added flexibility. The exchange-correlation energy of a typical hybrid functional can be written as

$$E_{XC}^{\text{hybrid}} = aE_X^{\text{exact}} + (1 - a)E_X^{\text{approx}} + E_C^{\text{approx}}, \tag{1.30}$$

where $0 < a < 1$ is the mixing parameter. Some hybrids have additional parameters and consist of more than two components for exchange and/or more than one component for correlation.

1.3   Self-interaction error

One might expect density functional approximations to give exact solutions for those one-electron systems for which the exact analytical solutions of the Schrödinger equation

are available. Unfortunately, this is not the case. Consider an example—the hydrogen atom. Clearly, since it contains only one electron, there cannot be any electron-electron interactions. However, the total energy functional, $E[\rho] = T_s[\rho] + V[\rho] + J[\rho] + E_{\mathrm{XC}}[\rho]$, still contains an electron-electron repulsion term $J[\rho]$, which is written as

$$J[\rho] = \frac{1}{2} \int \int \frac{\rho(\mathbf{r})\rho(\mathbf{r}')}{|\mathbf{r} - \mathbf{r}'|} d\mathbf{r} d\mathbf{r}'. \tag{1.31}$$

Even in a one-electron system, $J[\rho]$ does not vanish because it contains a spurious interaction of electron density with itself. The exchange-correlation energy functional also deals with electron-electron interactions. Thus, the erroneous self-repulsion would not be an issue if it was cancelled out by $E_{\mathrm{XC}}[\rho]$. That is, for a DFA to be free of the *one-electron self-interaction error* (SIE), it should satisfy

$$E_{\mathrm{XC}}[\rho] = -J[\rho] \tag{1.32}$$

for any one-electron density. Common exchange-correlation functionals are not constructed to cancel out self-repulsion. The SIE leads to a number of qualitative and quantitative errors, including dissociation of polar molecules into fractionally charged species [18–24], underestimation of reaction barriers [25, 26], and errors in the description of charge-transfer complexes [27, 28].

One can eliminate the one-electron SIE by applying a self-interaction correction (SIC) scheme, such as the one by Perdew and Zunger [29]. This correction explicitly enforces Eq. 1.32 and helps to correct the problems associated with the SIE in atoms. However, the Perdew-Zunger correction not only leads to computational difficulties, but also tends to deteriorate the performance on thermochemistry [30].

There exist functionals that satisfy Eq. 1.32 [31, 32]. However, these functionals include 100% of the exact exchange, and the combination of $E_{\mathrm{X}}^{\mathrm{exact}}$ with an approximate correlation term results in poor accuracy. Moreover, even with the functionals free from the one-electron SIE, some difficulties related to self-interaction remain, because correct results in the one-electron case do not mean there is no self-interaction in many-electron systems. The latter is usually referred to as the *many-electron self-interaction error*.

1.4   Derivative discontinuity in DFT

While there is no such thing as a fractionally charged atom or molecule in nature, one may encounter fractional electron numbers in DFT when dealing with a time average of

an open system, e.g. atom X which can exchange electrons with atom Y. Such a system is represented in quantum mechanics by an ensemble average of states with integer electron numbers. The resulting energy E is a function of the average number of electrons, N. For a system with the number of electrons fluctuating between the integers J and $(J+1)$, and with the probability of the $(J+1)$-electron state p, the average energy becomes

$$E = (1 - p)E_J + pE_{J+1}, \qquad (1.33)$$

where E_J and E_{J+1} are the ground-state energies for the J- and $(J+1)$-electron systems. The average number of electrons is $N = J + p$. Eq. 1.33 suggests that the curve of E versus N in exact DFT is linear between a pair of neighbouring integer electron numbers. In other words, the curve consists of a series of straight-line segments [18, 33].

Now, consider the derivative of the total energy E with respect to the electron number N. From the piecewise-linear shape of $E(N)$, the derivative $\partial E/\partial N$ must be constant within the straight-line segments, and it must have discontinuities at integer values of N. It was shown by Janak [34] that, in both exact and approximate DFT,

$$\frac{\partial E}{\partial N} = \varepsilon_i, \qquad (1.34)$$

where ε_i is the eigenvalue of the orbital whose occupation is varying. So, $\partial E/\partial N$ gives the set of orbital eigenvalues and jumps by a constant as N passes an integer. This property of exact DFT is called *derivative discontinuity* [18].

The values of $\partial E/\partial N$ at the points where N passes through the number of electrons M in a neutral system are of particular interest. In exact DFT they correspond to the first ionization energy I and the electron affinity A of that M-electron system:

$$\varepsilon_i(M - 1 < N < M) = \varepsilon_M = -I_M, \qquad (1.35)$$

$$\varepsilon_i(M < N < M + 1) = \varepsilon_{M+1} = -A_M, \qquad (1.36)$$

Approximate DFT lacks piecewise linearity and, consequently, derivative discontinuity. Lack of derivative discontinuity is closely associated with the presence of the SIE: both problems lead to the same physical effects, but seem to explain these effects from different perspectives [33].

While at integer values of N the curve of E versus N for a common density functional comes very close to the exact one, the segments and the whole curve is convex (Fig. 1.1). Thus, the derivative $\partial E/\partial N$ is continuous and is not constant within the segments. The Janak's theorem (Eq. 1.34), which relates this derivative to the orbital eigenvalues,
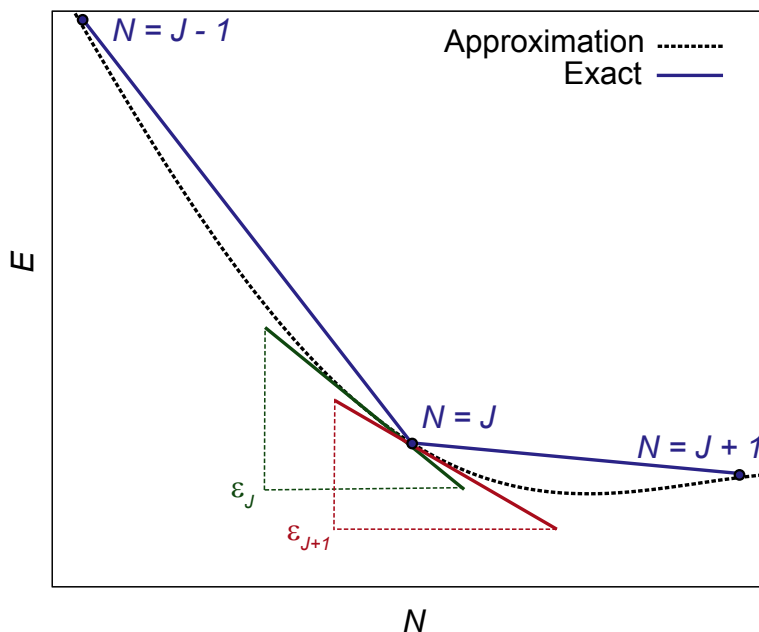
Figure 1.1: Typical dependence of the exact total energy of a system on the number of electrons and the energy calculated with a DFA. J is an integer. The exact curve consists of linear segments, whereas the approximate one is convex within these segments.

still holds, but these eigenvalues are far from the true ionization potentials and electron affinities. In Fig. 1.1, the slope of the tangent line to the approximate curve at the electron-deficit left-hand side of $N = J$ is equal to the energy of the J-th orbital, ε_J, and the slope of the tangent line at the electron-abundant right-hand side of $N = J$ is equal to the energy of the $(J + 1)$-th orbital, ε_{J+1}.

Compare these two slopes, ε_J and ε_{J+1}, to the slopes of the exact linear segments. The approximate ε_J is, in general, less negative than it should be, i.e. the binding energy of the electron occupying the J-th orbital is underestimated. The J-th orbital is in fact the highest occupied molecular orbital (HOMO) of the J-electron system, and the underestimation of its energy can lead to qualitatively incorrect predictions of electron removal energies. On the contrary, the approximate ε_{J+1} is much more negative than its exact counterpart. In the J-electron system, the $(J + 1)$-th orbital corresponds to the lowest unoccupied molecular orbital (LUMO), thus, HOMO-LUMO band gaps calculated using common semilocal density functionals are severely underestimated [35].

1.5 Asymptotic shape of the exchange-correlation potential

Recall that the exchange-correlation potential, v_{XC}, is a functional derivative of the exchange-correlation energy, E_{XC}, with respect to the electron density, ρ:

$$v_{XC}([\rho]; \mathbf{r}) = \frac{\delta E_{XC}[\rho]}{\delta \rho(\mathbf{r})}. \tag{1.37}$$

Direct modelling of v_{XC} is an alternative route to devise a new DFA. But even if a density functional is designed in a regular way, by building a E_{XC}, analysis of the shape of the exchange-correlation potential is a useful tool to explain or predict the performance of that functional.

The two common problems of popular density functionals, the self-interaction error and the lack of derivative discontinuity, are both reflected in the intermediate- and long-range shape of v_{XC} [36]. In order to avoid self-interaction, every electron in an N-electron system should only feel the potential of the rest of $(N-1)$ electrons. The Hartree potential for the chosen electron,

$$v_{H}([\rho]; \mathbf{r}) = \int \frac{\rho(\mathbf{r}')}{|\mathbf{r} - \mathbf{r}'|} d\mathbf{r}', \tag{1.38}$$

is known to fall off as N/r. It follows that to obtain an overall $(N-1)/r$ decay, the exchange-correlation potential should behave asymptotically as $-1/r$. In reality, the exchange-correlation potentials of typical semilocal functionals decay much faster (exponentially), so that the resulting Hartree-exchange-correlation potential, v_{HXC}, is too repulsive at intermediate and large r. The asymptotic shape of the exchange-correlation potentials is improved upon by adding a fraction of the exact exchange, since the HF exchange itself shows correct $-1/r$ decay. Thus, in hybrid functionals v_{XC} falls off as $-a/r$, where $0 < a < 1$ is the amount of the incorporated exact exchange [37].

The situation with the derivative discontinuity in terms of v_{XC} is more complicated. It was shown by Perdew *et al.* [18], that since the exact total energy is a piecewise-linear function of the electron number N, the exact exchange-correlation potential must be discontinuous at integer values of N with the electron-deficient and the electron-abundant sides differing by a system-dependent constant.

In practice one has to deal with continuous exchange-correlation potentials. Even with continuous potentials, one can still obtain accurate results given the correct asymptotic behavior of v_{XC}:

$$v_{XC}([\rho]; \mathbf{r}) \sim -\frac{1}{r} \quad (r \to \infty). \tag{1.39}$$

13

The incorrect asymptotic shape of v_{XC} has little influence on the occupied orbitals [38]. Therefore, properties that depend only on the occupied orbitals—total energies, ionization potentials, and molecular geometries—turn out to be of reasonable quality. As for the properties determined by the unoccupied orbitals—vertical excitation energies and polarizabilities—their accuracy is rather low [39, 40].

1.6 Objectives of the research

The main goal of this research was to tackle problems caused by the self-interaction error and the lack of derivative discontinuity in DFAs. Two examples of such problems are unphysical dissociation of polar molecules into fractionally charged species and underestimation of Rydberg vertical excitation energies in time-dependent DFT. In order to treat these two issues, we employ the concept of a fractionally charged system. A fractionally charged system can have either a non-integer number of electrons or partial nuclear charge. In Chapter 1, we devise a technique that enforces integer charges upon dissociation. The main idea of the technique is to model a corrected exchange-correlation potential for a system by fractionally depopulating its HOMO or populating the LUMO. In Chapter 2 we explore the possibility of using a slightly different approach to construct a model exchange-correlation potential. The fractionally charged system in this approach is obtained by adding a portion of nuclear charge. We employ this potential to calculate Rydberg excitation energies and compare the results to the performance of the fractional HOMO depopulation method.

Bibliography

[1]   A. Szabo and N. S. Ostlund, *Modern Quantum Chemistry: Introduction to Advanced Electronic Structure Theory* (McGraw-Hill, New York, 1989).

[2]   D. R. Hartree, "The wave mechanics of an atom with a non-coulomb central field. Part I. Theory and methods", Math. Proc. Cambridge Phil. Soc. **24**, 89–110 (1928).

[3]   V. Fock, "Näherungsmethode zur Lösung des quantenmechanischen Mehrkorper-problems", Z. Phys. **61**, 126–148 (1930).

[4]   C. Møller and M. S. Plesset, "Note on an approximation treatment for many-electron systems", Phys. Rev. **46**, 618–622 (1934).

[5]   J. Čížek, "On the correlation problem in atomic and molecular systems. Calculation of wavefunction components in Ursell-type expansion using quantum-field theoretical methods", J. Chem. Phys. **45**, 4256–4266 (1966).

[6]   D. Hegarty and M. A. Robb, "Application of unitary group methods to configuration interaction calculations", Mol. Phys. **38**, 1795–1812 (1979).

[7]   R. A. Friesner, "*Ab initio* quantum chemistry: Methodology and applications", Proc. Natl. Acad. Sci. USA **102**, 6648–6653 (2005).

[8]   P. Hohenberg and W. Kohn, "Inhomogeneous electron gas", Phys. Rev. **136**, B864–B871 (1964).

[9]   W. Koch and M. C. Holthausen, *A Chemist's Guide to Density Functional Theory*, 2nd ed. (Wiley-VCH, Weinheim, 2001).

[10] R. G. Parr and W. Yang, *Density-Functional Theory of Atoms and Molecules* (Oxford University Press, New York, 1998).

[11] M. Levy, "Universal variational functionals of electron densities, first-order density matrices, and natural spin-orbitals and solution of the v-representability problem", Proc. Natl. Acad. Sci. USA **76**, 6062–6065 (1979).

[12] E. H. Lieb, "Density functionals for Coulomb systems", Int. J. Quant. Chem. **24**, 243–277 (1983).

[13] W. Kohn and L. J. Sham, "Self-consistent equations including exchange and correlation effects", Phys. Rev. **140**, A1133–A1138 (1965).

[14] F. Bloch, "Bemerkung zur Elektronentheorie des Ferromagnetismus und der elektrischen Leitfähigkeit", Z. Phys. **57**, 545–555 (1929).

[15] P. A. M. Dirac, "Note on exchange phenomena in the Thomas atom", Math. Proc. Cambridge Philos. Soc. **26**, 376–385 (1930).

[16] P. Jemmer and P. J. Knowles, "Exchange energy in Kohn-Sham density-functional theory", Phys. Rev. A **51**, 3571–3575 (1995).

[17] G. E. Scuseria and V. N. Staroverov, "Progress in the development of exchange-correlation functionals", in *Theory and Applications of Computational Chemistry*, edited by G. E. Scuseria, C. E. Dykstra, G. Frenking, and K. S. Kim (Elsevier, Amsterdam, 2005), pp. 669–724.

[18] J. P. Perdew, R. G. Parr, M. Levy, and J. L. Balduz, "Density-functional theory for fractional particle number: Derivative discontinuities of the energy", Phys. Rev. Lett. **49**, 1691–1694 (1982).

[19] A. Ruzsinszky, J. P. Perdew, G. I. Csonka, O. A. Vydrov, and G. E. Scuseria, "Spurious fractional charge on dissociated atoms: Pervasive and resilient self-interaction error of common density functionals", J. Chem. Phys. **125**, 194112 (2006).

[20] A. D. Dutoi and M. Head-Gordon, "Self-interaction error of local density functionals for alkali-halide dissociation", Chem. Phys. Lett. **422**, 230–233 (2006).

[21] O. A. Vydrov, G. E. Scuseria, and J. P. Perdew, "Tests of functionals for systems with fractional electron number", J. Chem. Phys. **126**, 154109 (2007).

[22] J. P. Perdew, A. Ruzsinszky, G. I. Csonka, O. A. Vydrov, G. E. Scuseria, V. N. Staroverov, and J. Tao, "Exchange and correlation in open systems of fluctuating electron number", Phys. Rev. A **76**, 040501 (2007).

[23] A. Makmal, S. Kümmel, and L. Kronik, "Dissociation of diatomic molecules and the exact-exchange Kohn-Sham potential: The case of LiF", Phys. Rev. A **83**, 062512 (2011).

[24] E. Kraisler and L. Kronik, "Elimination of the asymptotic fractional dissociation problem in Kohn-Sham density-functional theory using the ensemble-generalization approach", Phys. Rev. A **91**, 032504 (2015).

[25] B. G. Johnson, C. A. Gonzales, P. M. Gill, and J. A. Pople, "A density functional study of the simplest hydrogen abstraction reaction. Effect of self-interaction correction", Chem. Phys. Lett. **221**, 100 –108 (1994).

[26] L. Deng, V. Branchadell, and T. Ziegler, "Potential energy surfaces of the gas-phase S_N2 reactions $X^- + CH_3X = XCH_3 + X^-$ (X = F, Cl, Br, I): A comparative study by density functional theory and *ab initio* methods", J. Am. Chem. Soc. **116**, 10645–10656 (1994).

[27] D. J. Tozer, "Relationship between long-range charge-transfer excitation energy error and integer discontinuity in Kohn-Sham theory", J. Chem. Phys. **119**, 12697–12699 (2003).

[28] C. Toher, A. Filippetti, S. Sanvito, and K. Burke, "Self-interaction errors in density-functional calculations of electronic transport", Phys. Rev. Lett. **95**, 146402 (2005).

[29] J. P. Perdew and A. Zunger, "Self-interaction correction to density-functional approximations for many-electron systems", Phys. Rev. B **23**, 5048–5079 (1981).

[30] O. A. Vydrov and G. E. Scuseria, "Effect of the Perdew-Zunger self-interaction correction on the thermochemical performance of approximate density functionals", J. Chem. Phys. **121**, 8187–8193 (2004).

[31] D. Becke A, "Real-space post-Hartree-Fock correlation models", J. Chem. Phys. **122**, 064101 (2005).

[32] P. Mori-Sánchez, A. J. Cohen, and W. Yang, "Self-interaction-free exchange-correlation functional for thermochemistry and kinetics", J. Chem. Phys. **124**, 091102 (2006).

[33] J. P. Perdew, "Size-consistency, self-interaction correction, and derivative discontinuity in density functional theory", in *Density Functional Theory of Many-Fermion Systems*, edited by P.-O. Löwdin (Academic Press, 1990), pp. 113 –134.

[34] J. F. Janak, "Proof that $\partial E/\partial n_i = \epsilon$ in density-functional theory", Phys. Rev. B **18**, 7165–7168 (1978).

[35] J. P. Perdew, "Density functional theory and the band gap problem", Int. J. Quant. Chem. **28**, 497–523 (1985).

[36] T. Schmidt, E. Kraisler, L. Kronik, and S. Kummel, "One-electron self-interaction and the asymptotics of the Kohn-Sham potential: An impaired relation", Phys. Chem. Chem. Phys. **16**, 14357–14367 (2014).

[37] M. E. Casida, "Time-dependent density functional response theory of molecular systems: Theory, computational methods, and functionals", in *Recent Developments and Applications of Modern Density Functional Theory*, Vol. 4, edited by J. M. Seminario (Elsevier, 1996), pp. 391–439.

[38] D. J. Tozer and N. C. Handy, "The development of new exchange-correlation functionals", J. Chem. Phys. **108**, 2545–2555 (1998).

[39] M. Petersilka, U. J. Gossmann, and E. K. U. Gross, "Excitation energies from time-dependent density-functional theory", Phys. Rev. Lett. **76**, 1212–1215 (1996).

[40] M. E. Casida, C. Jamorski, K. C. Casida, and D. R. Salahub, "Molecular excitation energies to high-lying bound states from time-dependent density-functional response theory: Characterization and correction of the time-dependent local density approximation ionization threshold", J. Chem. Phys. **108**, 4439–4449 (1998).

Chapter 2

Elimination of spurious fractional charges in dissociating molecules by correcting the shape of approximate Kohn-Sham potentials

2.1 Introduction: Dissociation of diatomic molecules

Consider the dissociation of a polar diatomic molecule XY (where Y denotes the more electronegative atom). Specifically, we are interested in how the charges on X and Y change when the molecule is stretched and whether the neutral atoms or the pair of ions, X^+ and Y^-, are the product of dissociation.

In the beginning, when the internuclear distance is still close to the equilibrium bond length $R_e(X–Y)$, the atoms are ionized since the electrostatic attraction energy between X^+ and Y^- is high enough to compensate for the energy required to ionize them. This energy is just the difference between the ionization energy of X and the electron affinity of Y, $(I_X - A_Y)$, and here we assume that it is always positive.

As the molecule is stretched further, the Coulomb attraction energy decreases as $1/R$, while $(I_X - A_Y)$ stays constant. Consequently, at some point the Coulomb energy drops below the energy needed to produce the pair of ions, and the two neutral atoms become the more favorable state. The internuclear separation at which this interchange occurs for a given molecule is called the *critical radius*, R_c:

$$R_c(XY) = \frac{e^2}{I_X - A_Y}.$$
(2.1)

If the molecule is stretched to infinite internuclear distance, the Coulomb energy vanishes, so the molecule stays in its neutral state.

In the discussion above, we assumed that energy is always consumed when X and Y are ionized to obtain X^+ and Y^-, that is, $(I_X - A_Y)$ is positive. Let us now verify that this is true for any pair of elements from the periodic table. It is known that the lowest ionization energy is that of cesium, $I_{Cs} = 3.89$ eV, and the highest electron affinity belongs to chlorine, $A_{Cl} = 3.61$ eV. So, even the smallest energy that is required to produce an ionized pair, $(I_{Cs} - A_{Cl}) = 0.28$ eV, is positive. This confirms that in any fully ionic diatomic molecule the correct charges on atoms are ± 1 at $R_{X-Y} < R_c(XY)$ and zero at $R_{X-Y} > R_c(XY)$, the dissociation product is always a pair of neutral atoms.

2.2 Theory

2.2.1 Tests of DFAs for fractional charge dissociation problem

Unfortunately, the majority of DFAs currently in use fail to predict correct dissociation products. Instead, they dissociate diatomic molecules into unphysical fractionally charged atoms [1–7].

The major cause of this is the lack of derivative discontinuity. DFAs produce the total energy E that is convex within the segments $(J - 1) < N < J$ (Fig. 1.1). Due to the convexity of $E(N)$, approximate semi-local functionals overestimate eigenvalues of the HOMOs and severely underestimate eigenvalues of the LUMOs. For many pairs of elements, the orbital energies of the frontier orbitals are off to such an extent that $\epsilon^{LUMO}(Y) < \epsilon^{HOMO}(X)$, where atom Y is more electronegative than X. This does not happen in reality, even for the pairs of X and Y with the largest differences in electronegativities. If $\epsilon^{LUMO}(Y) < \epsilon^{HOMO}(X)$, then a fraction of an electron can be transferred from X to Y. The two atomic fragments go from neutral atoms to fractionally charged species $X^{+q'}$ and $Y^{-q'}$, where $0 \leq q' < 1$, and the energy change in such a process is negative:

$$\Delta E = (\epsilon^{LUMO}(Y) - \epsilon^{HOMO}(X))\delta q' < 0. \tag{2.2}$$

If the eigenvalue of the HOMO of the partially charged fragment $X^{+q'}$ is still higher then the eigenvalue of the LUMO of $Y^{-q'}$ (which is, strictly speaking, not the LUMO anymore, since it is fractionally populated), the process continues. The charge transfer stops when at some $q' = q$ the eigenvalues of the frontier orbitals equalize. Thus, an attempt to find the lowest-energy solution via the self-consistent procedure results in fractionally charged fragments. According to Ruzsinszky *et al.*, fractional charges are observed for 174 of 276

diatomic molecules made of the first 24 open *sp*-shell atoms [2].

Two examples of such diatomic molecules are LiF and SiO. For these molecules we tested the accuracy of charges calculated with four common DFAs: the local density approximation (LDA), the generalized gradient approximation by Perdew, Burke, and Ernzerhof (PBE) [8], the meta-GGA by Tao, Perdew, Staroverov, and Scuseria (TPSS) [9], and the hybrid functional constructed from PBE (PBE0) [10]. Each of these functionals is typical of its rung in the ladder of density functional approximations [11]. Thus, one can expect the charges calculated with other GGAs, meta-GGAs, and hybrids to be very similar to the ones predicted by the PBE, TPSS, and PBE0 functionals respectively. The results obtained with two methods that enforce correct integer charge dissociation, the Hartree-Fock method and the long-range corrected hybrid PBE functional (LC-ωPBE) [12], are included for comparison. In the HF method, the states with fractional numbers of electrons are energetically unfavourable, since the ground-state energy E in this method is concave inside the segments $(J-1) < N < J$. Despite predicting correct charges, the HF approximation is not appropriate for chemical applications because of significant errors introduced by neglecting electron correlation. The errors in thermochemical properties are especially large: on a test set of 32 molecules composed of first- and second-row elements, the mean absolute deviation between atomization energies computed with the HF method (6-31G(d) basis set) and experiment turned out to be 86 kcal/mol [13]. Of course, accurate wavefunction-based approximations, such as multi-configurational self-consistent field and coupled cluster theory, dissociate molecules correctly, but they are computationally demanding.

Within the DFT framework, range-separated hybrids, such as LC-ωPBE, which have improved asymptotic shape of the exchange-correlation potential, are one way of achieving correct dissociation behavior [4]. Other methods include eliminating the one-electron self-interaction error [14] and employing exact-exchange potentials [6].

The computations in this chapter were performed using a modified version of the Gaussian 03 [15] code and its newer version, Gaussian 09 [16], for the LC-ωPBE method. The calculations were unrestricted; the keyword Stable=Opt was used to ensure the lowest energy state was found in each case. UltraFine integration grid and 6-311+G(d) basis set were employed throughout unless otherwise specified.

Since in a molecule the densities of two atoms overlap, there is no unique definition for the charge on one of the atoms, therefore, various population analyses have to be used. They differ in the way the net charge is defined, but eventually, as the interatomic distance increases and the overlap between the densities becomes negligible, their results converge. We have used the natural population analysis (NPA) [17] to calculate charges.

In the NPA scheme, the charge on an atom is obtained as the sum of the occupation numbers of the natural atomic orbitals localized on this atom. The interatomic overlap between the natural orbitals of adjacent atoms is removed during their construction. The advantages of the natural population analysis are its stability with respect to basis set changes and better description of the charge distributions in ionic compounds.
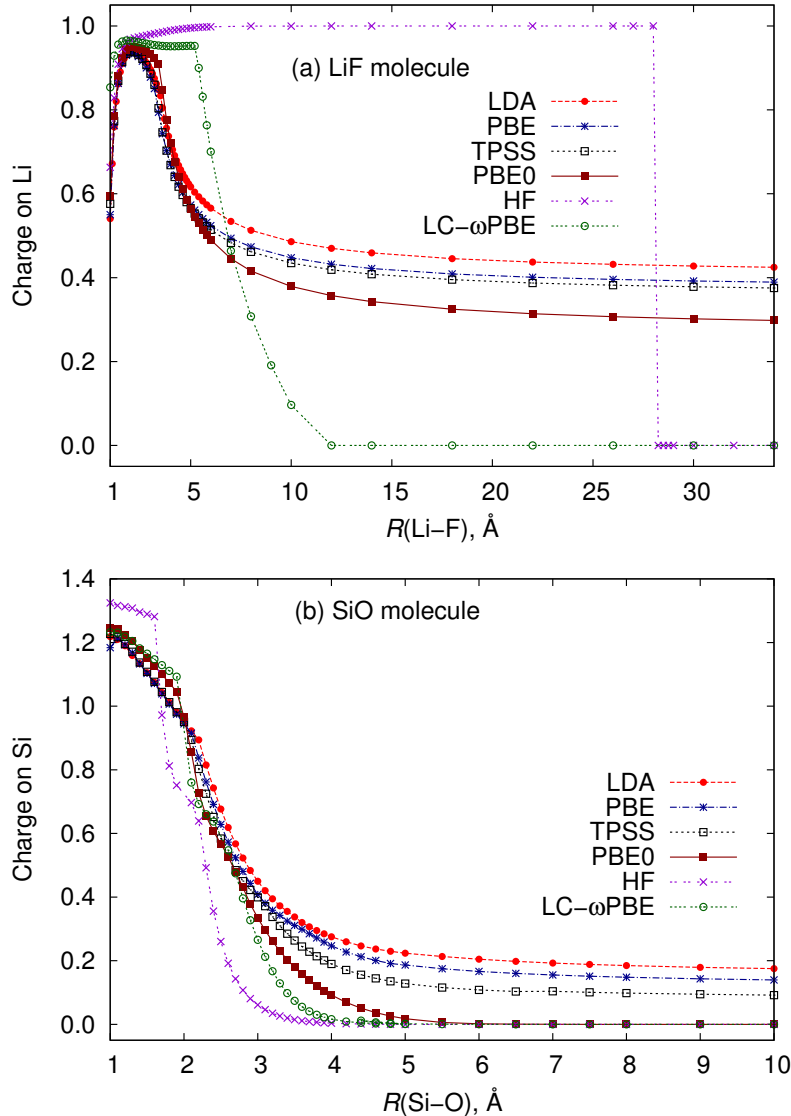

Figure 2.1: NPA charges on Li in LiF (a) and on Si in SiO (b) versus bond lengths. Fractional charges result from the calculations employing LDA, PBE and TPSS; The HF method and the LC-ωPBE functional give qualitatively correct curves; the hybrid PBE0 dissociates SiO correctly, but fails for LiF.

Figure 2.1 shows the NPA charges on Li atom in LiF (a) and on Si in SiO (b) as functions of the internuclear separations. For XY = LiF, from experimental data for $I(\text{Li})$

and A(F), R_{c}(LiF) $= 7.23\,\text{Å}$; and for SiO R_{c}(SiO) $= 2.15\,\text{Å}$. None of the methods succeeds in predicting R_{c}, but the curves calculated with the HF and the LC-ωPBE methods are qualitatively correct: large charge for separations close to the equilibrium distance drops quite suddenly to near zero. As for the LDA, PBE, and TPSS approximations, they predict that the charge on X tends to a nonzero limit ($\simeq 0.4$ for Li and $\simeq 0.1$ for Si) as $R \to \infty$. The hybrid PBE0 functional has the classical exchange term from the HF theory as an ingredient of its exchange-correlation functional. The incorporation of the exact exchange makes PBE0 behave in some aspects like the HF method, so it improves the charge on Si. But the charge on Li remains a challenge.

2.2.2 Correcting the shape of exchange-correlation potentials via fractional occupations

We propose a new correction scheme to enforce integer charge dissociation by changing the shape of the exchange-correlation potential. The scheme is based on the previous work by Gaiduk, Firaha, Mizzi, and Staroverov [18, 19], who showed that a more accurate Kohn-Sham potential of a system can be obtained by performing calculations with a fraction of an electron removed from that system. The correction scheme discussed in the present work is easy to implement, it has virtually no added computational cost, and it also improves other properties, such as eigenvalues of the highest occupied and the lowest unoccupied molecular orbitals and excitation energies.

Let us now examine how the introduction of fractional occupations affects the exchange-correlation potential. Recall that the exchange-correlation potential is a component of the Hartree-exchange-correlation potential:

$$v_{\mathrm{HXC}}([\rho]; \mathbf{r}) = v_{\mathrm{H}}([\rho]; \mathbf{r}) + v_{\mathrm{XC}}([\rho]; \mathbf{r}). \tag{2.3}$$

$v_{\mathrm{HXC}}([\rho]; \mathbf{r})$ arises from the electron-electron interactions in the system.

Now, consider an M-electron system of interest and an auxiliary system with a fractional number of electrons $(M + \omega)$. The density of the auxiliary system is

$$\tilde{\rho}(\mathrm{r}) = \rho(\mathrm{r}) + \omega|\phi_{\mathrm{FMO}}|^2, \tag{2.4}$$

where FMO stands for a frontier molecular orbital, either the HOMO or the LUMO, depending on the sign of ω.

To calculate the shape-corrected exchange-correlation potential $v_{\mathrm{XC}}^{\mathrm{corrected}}([\rho]; \mathbf{r})$, one
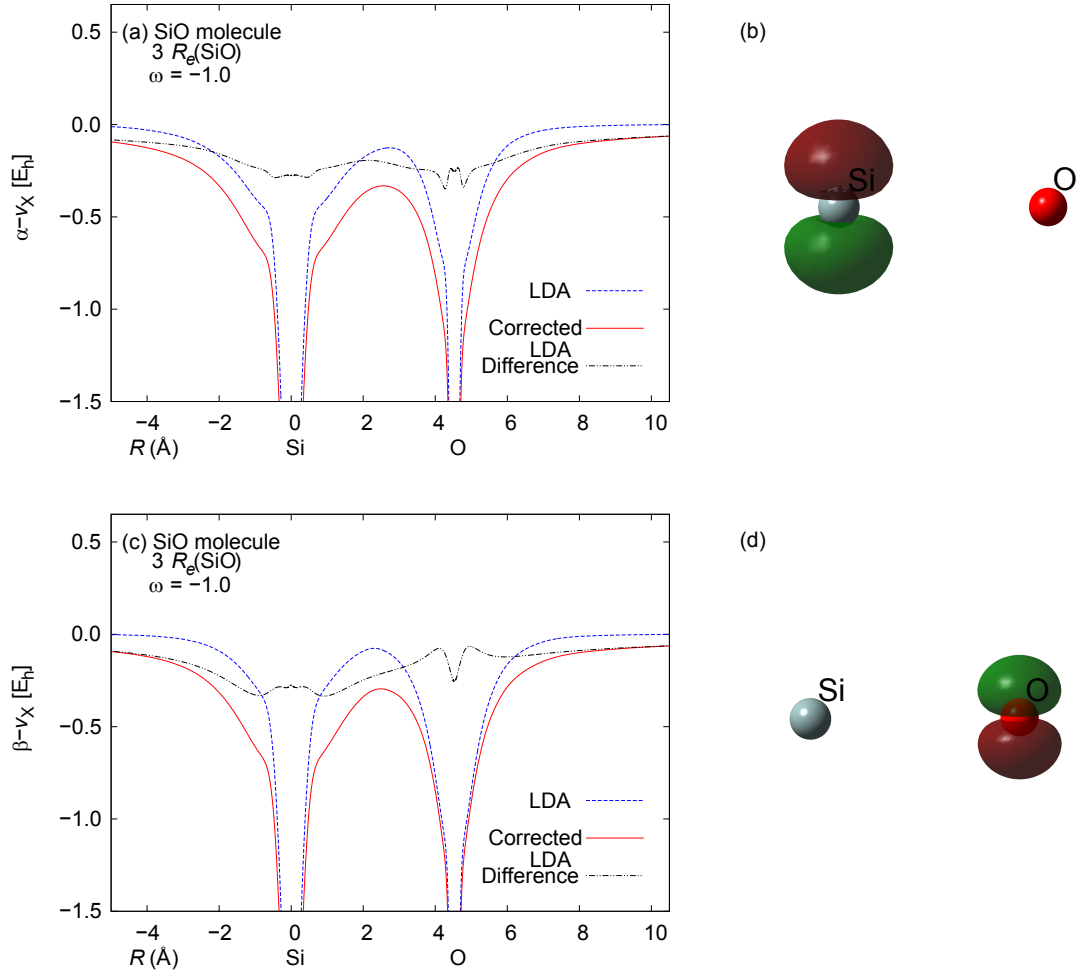
Figure 2.2: Self-consistent LDA exchange potentials of the SiO molecule at $R(\text{Si–O}) = 3R_e(\text{SiO})$ and the corresponding HOMOs: the potential evaluated for the spin-up density (a) and the spin-up HOMO (b), the potential evaluated for the spin-down density (c) and the spin-down HOMO (d). The potentials are calculated with aug-cc-pVQZ basis set using an integration grid with 599 radial shells and 974 points per shell. Corrected LDA potentials are obtained by fractionally depopulating the spin-up HOMO by 1.0 electron.

needs to replace $v_{\text{HXC}}([\rho]; \mathbf{r})$ in the Kohn-Sham equations,

$$\left[-\frac{1}{2}\nabla^2 + v(\mathbf{r}) + v_{\text{HXC}}([\rho]; \mathbf{r}) \right] \phi_i(\mathbf{r}) = \varepsilon_i \phi_i(\mathbf{r}), \tag{2.5}$$

with the Hartree-exchange-correlation potential of the auxiliary $(M + \omega)$-electron system, then solve the equations self-consistently, and calculate $v_{\text{XC}}^{\text{corrected}}([\rho]; \mathbf{r})$ as the difference
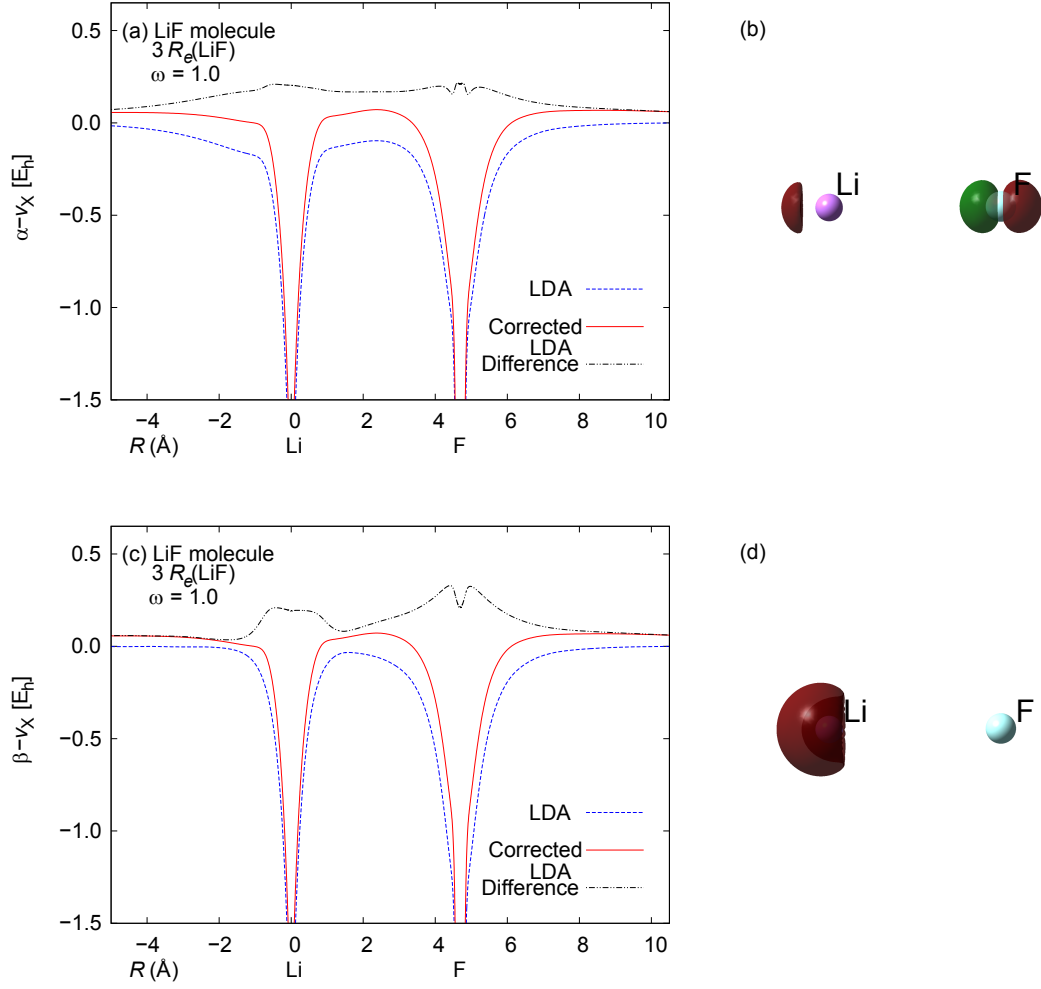
Figure 2.3: Self-consistent LDA exchange potentials of the LiF molecule at $R(\text{Li–F}) = 3R_e(\text{LiF})$ and the corresponding LUMOs: the potential evaluated for the spin-up density (a) and the spin-up LUMO (b), the potential evaluated for the spin-down density (c) and the spin-down LUMO (d). The potentials are calculated with aug-cc-pVQZ basis set using an integration grid with 599 radial shells and 974 points per shell. Corrected LDA potentials are obtained by fractionally populating the spin-up LUMO by 1.0 electron.

between $v_{\text{HXC}}([\tilde{\rho}]; \mathbf{r})$ and the Hartree potential of the initial M-electron system:

$$v_{\text{XC}}^{\text{corrected}}([\rho]; \mathbf{r}) = v_{\text{HXC}}([\tilde{\rho}]; \mathbf{r}) - v_{\text{H}}([\rho]; \mathbf{r}). \tag{2.6}$$

Let us now see how the initial exchange-correlation potential compares with the corrected one. The effect of the correction,

$$\Delta v_{\text{XC}}([\rho]; \mathbf{r}) = [v_{\text{XC}}([\tilde{\rho}]; \mathbf{r}) - v_{\text{XC}}([\rho]; \mathbf{r})] + [v_{\text{H}}([\tilde{\rho}]; \mathbf{r}) - v_{\text{H}}([\rho]; \mathbf{r})], \tag{2.7}$$
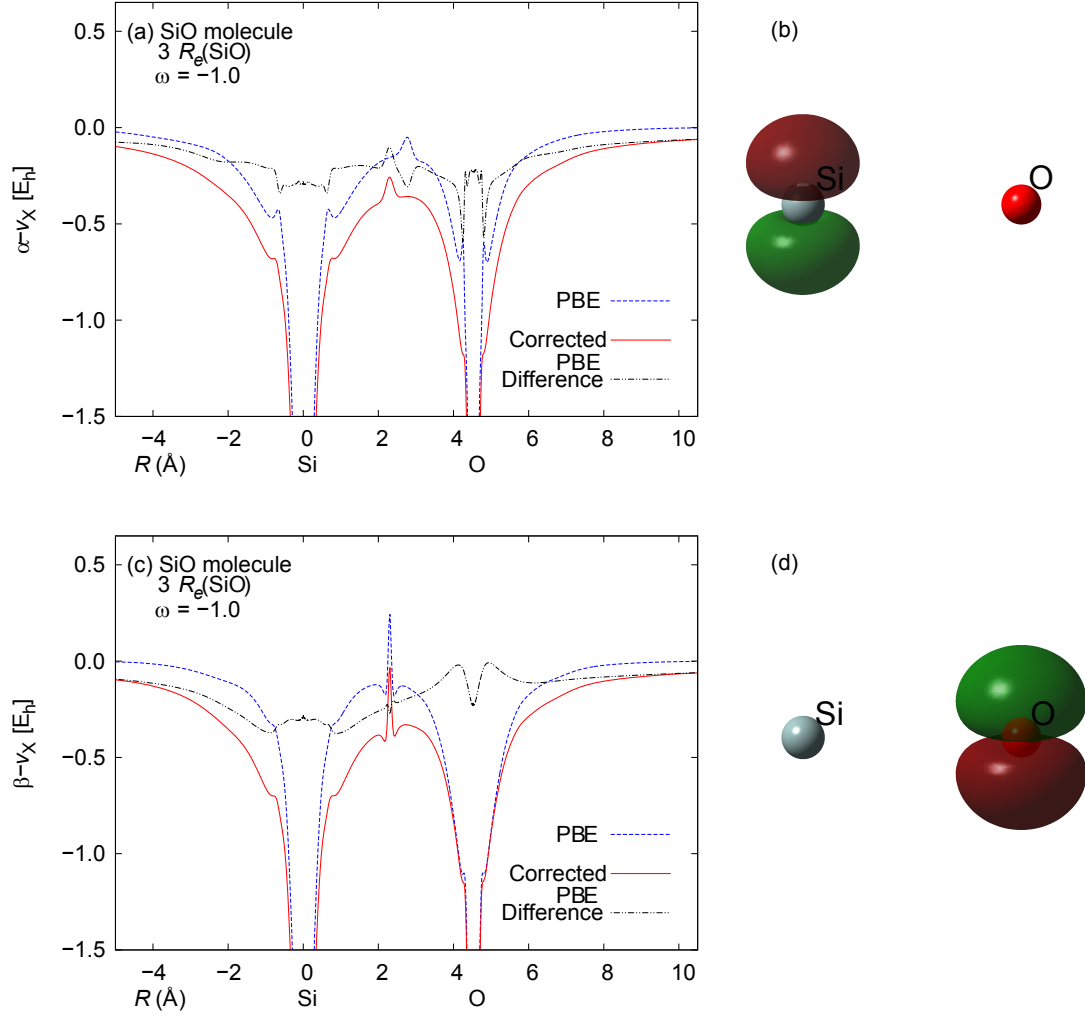
Figure 2.4: Self-consistent PBE exchange potentials of the SiO molecule at $R(\text{Si–O}) = 3R_e(\text{SiO})$ and the corresponding HOMOs: the potential evaluated for the spin-up density (a) and the spin-up HOMO (b), the potential evaluated for the spin-down density (c) and the spin-down HOMO (d). The potentials are calculated with aug-cc-pVQZ basis set using an integration grid with 599 radial shells and 974 points per shell. Corrected PBE potentials are obtained by fractionally depopulating the spin-up HOMO by 1.0 electron.

is determined by its sign, which in its turn depends on the sign of ω. If ω is negative (a fraction of an electron is removed), then $v_{\text{XC}}([\tilde{\rho}]; \mathbf{r})$ is less negative than $v_{\text{XC}}([\rho]; \mathbf{r})$, but this is counteracted by the decrease in $v_{\text{H}}([\tilde{\rho}]; \mathbf{r})$, which scales more rapidly with ρ. As a result, $v_{\text{HXC}}([\tilde{\rho}]; \mathbf{r}) < v_{\text{HXC}}([\rho]; \mathbf{r})$ and $\Delta v_{\text{XC}}([\rho]; \mathbf{r}) < 0$. Using the same reasoning, if ω is positive (a fraction of an electron is added), then $\Delta v_{\text{XC}}([\rho]; \mathbf{r}) > 0$. Thus, by applying fractional occupations we can either decrease or increase the exchange-correlation
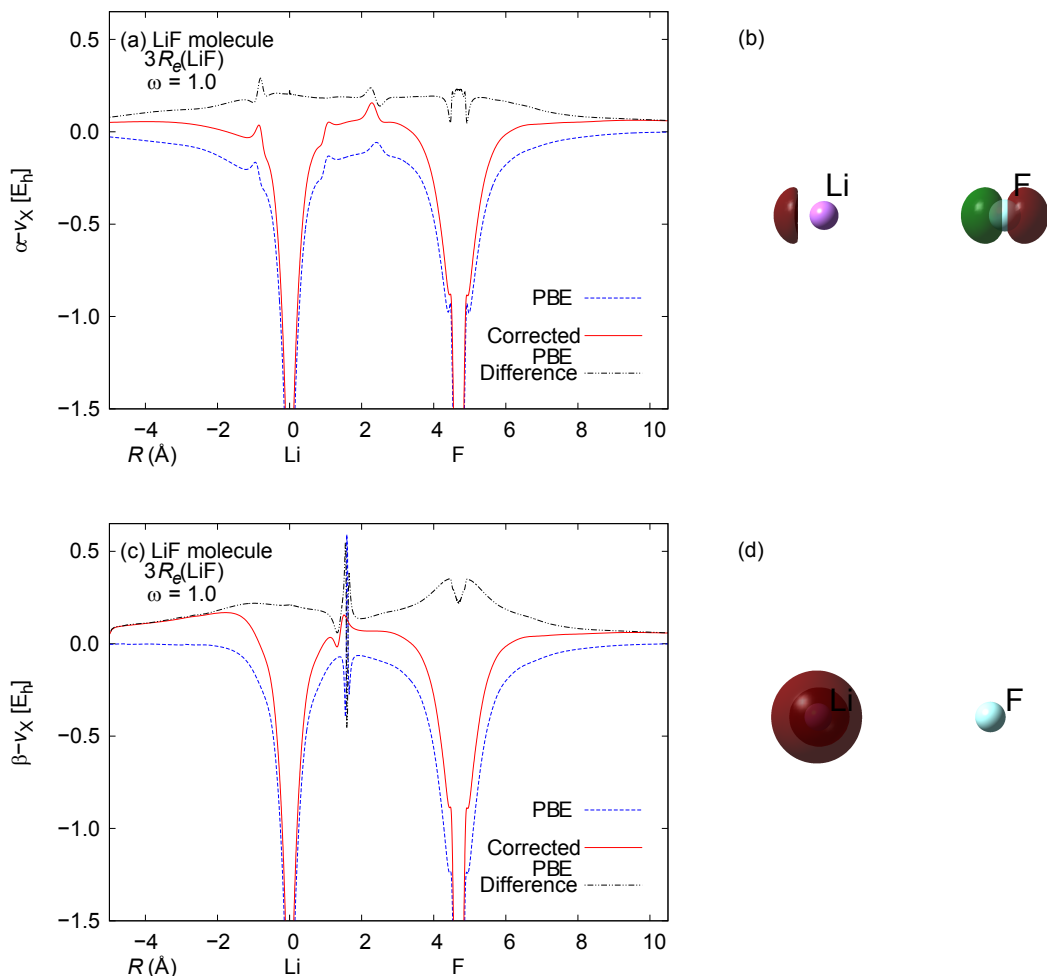
Figure 2.5: Self-consistent PBE exchange potentials of the LiF molecule at $R(\text{Li–F}) = 3R_e(\text{LiF})$ and the corresponding LUMOs: the potential evaluated for the spin-up density (a) and the spin-up LUMO (b), the potential evaluated for the spin-down density (c) and the spin-down LUMO (d). The potentials are calculated with aug-cc-pVQZ basis set using an integration grid with 599 radial shells and 974 points per shell. Corrected PBE potentials are obtained by fractionally populating the spin-up LUMO by 1.0 electron.

potential in the regions where the fractionally occupied orbital is localized. This is the key feature of the method, which allows one to correct the density distribution: the exchange-correlation potential does not change by the same amount everywhere in the molecule.

Let us explore two examples: the SiO molecule (Fig. 2.2), which requires the HOMO depopulation, and the LiF molecule (Fig. 2.3), which requires the LUMO population. In both of these cases we choose $\omega = \pm 1.0$ for illustration purposes, as it makes the

effect more pronounced compared to the effect of lower magnitudes of ω, and we use exchange-only LDA.

In SiO, we depopulate the α-HOMO. The depopulated orbital is localized on silicon, consequently, considering the total change in the α- and β-spin exchange potentials, the lowering of v_X is more pronounced in the vicinity of the Si nucleus. The electron density is forced to shift towards the region with lower v_X, and this density gain makes the charge on Si less positive.

In LiF, we populate the α-LUMO (the procedure to chose the orbital and the sign of ω is outlined in Section 2.2.3). This orbital is localized on fluorine, thus, the buildup of the potential in the vicinity of F is larger than in the vicinity of Li. The electron density flows towards Li, the magnitudes of charges decrease and become close to zero.

The overall effect of the correction on the exchange potentials in Fig. 2.2 and 2.3 (specifically, the spin-down potentials) is the shift of the potential wells of the more electronegative atoms, O and F, relative to the potential wells of the less electronegative atoms, Si and Li. A similar feature appears in exact DFT. The exact exchange-correlation potential of a polar diatomic molecule has step structure, that is, the potential is upshifted near the atom with the higher ionization energy [20–22]. Thus, the corrected potentials mimics the step structure of the exact v_{XC}.

The potentials obtained from the exchange-only PBE functional and their corrected counterparts (Fig. 2.4 for SiO and Fig. 2.5 for LiF) are similar to the LDA potentials of Fig. 2.2 and 2.3. Note that the spikes in the interatomic regions in Fig. 2.5 and 2.4 are not related to the method of fractional occupations, they are a feature of the PBE exchange potential. To explain the spikes we refer to the analytic representation of the exchange potential v_X of a generalized gradient approximation [23],

$$
\begin{aligned}
v_X =& \frac{\partial f}{\partial \rho} + \frac{4}{3}\frac{\partial^2 f}{\partial s^2}\frac{s^2}{\rho} - \frac{\partial^2 f}{\partial \rho \partial s}s - \frac{\partial f}{\partial s}\frac{q}{\rho s} \\
& + \left(\frac{\partial f}{\partial s} - s\frac{\partial^2 f}{\partial s^2}\right)\frac{u}{\rho s^3},
\end{aligned}
\tag{2.8}
$$

where s, q, and u are dimensionless counterparts of the density gradient, Laplacian, and Hessian, f is the energy-density function. The expression for the PBE potential derived via Eq. 2.8 is a sum in which each of the terms depends on ρ and s, some depend on q and u.

In the region between two nuclei there is a point at which the density, ρ, has a minimum, the reduced density gradient, s, is zero and also has a minimum, q has a maximum, u is zero and has a minimum. Substituting these extremum values of ρ, s,

q, and u into the expression for the PBE exchange potential results in extremum values of the summands. The summands do not cancel each other out, so the potential has a spike. A detailed explanation is given in Appendix A.

2.2.3 Fractional occupation technique

In this section we outline the detailed procedure to follow in order to obtain qualitatively correct charges in a polar molecule XY.

As discussed previously, the effect of our method relies on the choice of orbital to be fractionally occupied. Thus, given a stretched molecule with two spin-HOMOs and two spin-LUMOs, the first block of steps is to decide which one of these orbitals should be either depopulated or populated. This is done according to the following algorithm:

1. To determine the sign of ω, i.e. choose between the HOMO and the LUMO, perform unrestricted self-consistent calculations on the XY^+ cation, the XY^- anion, and the neutral XY molecule. Use the orbitals of XY^+ and XY^- to estimate the charge on X in the neutral molecule in post-SCF fashion, that is, by performing just one cycle of the SCF procedure (Fig. 2.6). The cation and the anion represent the cases of $\omega = -1$ (HOMO depopulation) and $\omega = 1$ (LUMO population) respectively, therefore, choose the sign of ω that has the desired effect of the charge on X, i.e., lowers the charge. If the charge is lowered in both cases, depopulate the HOMO.

2. If ω is negative, determine which of the two spin-HOMOs should be depopulated. If XY is an open-shell molecule, choose the majority spin HOMO (α-HOMO). Otherwise, choose the actual HOMO, that is, the one with the higher energy.

3. If ω is positive, the easiest way to fractionally populate the LUMO is to take the orbitals of the anion and remove $(1 - \omega)$ of an electron from its HOMO. The choice of the spin-HOMO to depopulate is exactly the same as above: if XY^- is open-shell, depopulate the α-HOMO, otherwise, depopulate the HOMO with the higher eigenvalue.

The second block of steps is to find the optimal fraction of an electron to remove or add. While a wide range of ω values for a particular molecule can lower the charges in it, a too high or too low ω may lead to an overcorrection, i.e., significant negative charge on X, or an undercorrection in addition to having poor SCF convergence. Therefore, an optimal ω value should be used.

4. Recall that in step 1 the decision was made on whether one should depopulate the HOMO and thus make the system closer to the cation, or populate the LUMO and
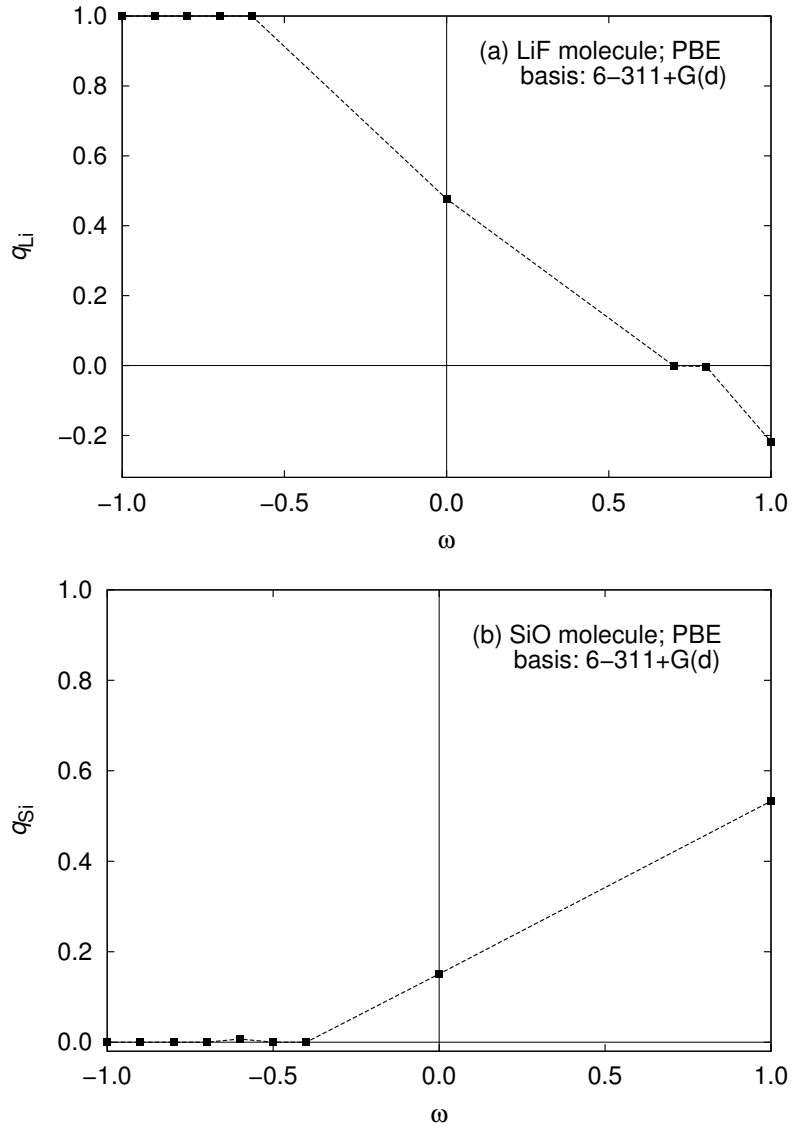
Figure 2.6: Post-SCF charges on Li in LiF (a) and on Si in SiO (b). In each case, the input orbitals for the post-SCF calculation are those of the corresponding cations ($\omega = -1.0$) and anions ($\omega = 1.0$).

Table 2.1: Quantities needed to estimate the optimal ω value via Eq. (2.9) for a diatomic molecule XY, where Y denotes a more electronegative atom.

	XY	XY$^+$	XY$^-$
Charge from a DFA	q_0	q_+	q_-
Correct charge	$q_0^{\text{correct}} = 0$	$q_+^{\text{correct}} = 1$	$q_-^{\text{correct}} = 0$
Error in charge	$\Delta q_0 = q_0 - 0$	$\Delta q_+ = q_+ - 1$	$\Delta q_- = q_- - 0$

make the system closer to the anion. Now, consider the charge on atom X in the appropriate ion, as well as the charge on X in the neutral molecule. For these two cases calculate the errors in charge on atom X (Table 2.1) obtained with DFAs as compared to the physically correct charges: X^0Y^0 for a neutral molecule, $X^{+1}Y^0$ for a cation, and X^0Y^{-1} for an anion. Once the values of Δq_0 and either Δq_+ or Δq_- from Table 2.1 are available, do a two-point interpolation to find ω:

$$\omega = \pm \frac{\Delta q_0}{\Delta q_\pm - \Delta q_0}. \tag{2.9}$$

A graphical representation of the interpolation for the LiF and SiO molecules is shown in Fig. 2.7.
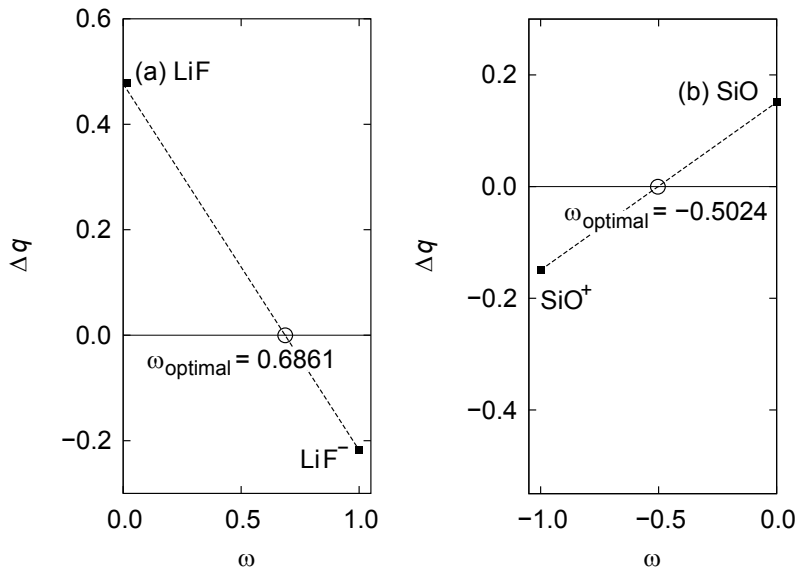
Figure 2.7: Two-point interpolation to find optimal values of ω for the LiF (a) and SiO (b) molecules stretched to 5 times the equilibrium internuclear distance at PBE/6-311+G(d) level of theory.

Once the four preliminary steps are completed, one can proceed to do the calculation on the fractionally occupied system.

5. Do a self-consistent calculation on the XY system with fractional electron number. The code for DFT calculations on such systems was implemented in the Gaussian 03 [15] package. The modified version takes standard Gaussian input with added control options for the fraction of an electron ω to be removed from either the spin-up or the spin-down HOMO. To fractionally occupy one of the spin-LUMOs

one can depopulate the HOMO of the corresponding anion by a $(1 - \omega)$ fraction of an electron.

6. Finally, use the orbitals from the previous step to evaluate energies, potentials, and charges by performing just one cycle of the self-consistent-field procedure.

Note that the choice of the sign of ω and the spin-orbital to fractionally occupy (the first three steps of the procedure above) should only be done once for a given molecule and that these calculations must be done for a stretched geometry, at which physical charges on X and Y are zeroes. However, one should calculate an optimal value of ω via Eq. 2.9 at every internuclear distance if one wants to explore charges upon dissociation.

2.3   Results

We explored how the charges on atoms change with increasing internuclear distance in the two example molecules, LiF and SiO. The results are plotted in Fig. 2.8, with the charges on Li and Si evaluated within the NPA framework. The most important feature of these curves is the correct dissociation limit: in both LiF and SiO the atoms are neutral at large R. Moreover, comparison of the two curves to the ones obtained using the HF and the LC-ωPBE methods in Fig. 2.1 shows that their overall shape is qualitatively correct: large charges for small separations drop suddenly to near-zero values as the internuclear distance increases. The bond lengths at which the charges drop to zero in Fig. 2.8 do not exactly match the experimental values of $R_c(\text{LiF}) = 7.23\,\text{Å}$ and $R_c(\text{SiO}) = 2.15\,\text{Å}$, but this is also the case with the HF and the LC-ωPBE in Fig. 2.1.

To further verify our findings, we have tested the method on a number of highly stretched diatomic molecules, both closed- and open-shell. Original charges calculated with three DFAs (PBE, TPSS, and PBE0) at 5 times the equilibrium internuclear separation are reported together with corrected charges and the corresponding (de)population parameters ω in Table 2.2. For all of the molecules in Table 2.2, the interatomic distance is larger than their critical radii. This corresponds to the rightmost side of Fig. 2.8 for LiF and SiO. Significant improvements are observed for all the molecules studied, as the corrected charges are essentially zeros. We have also tested the method of fractional occupations on a few examples of polyatomic molecules, and the resulting zero charges in BeF_2, BF_3, and CO_2 suggest that the method can be successfully applied to polyatomic molecules.
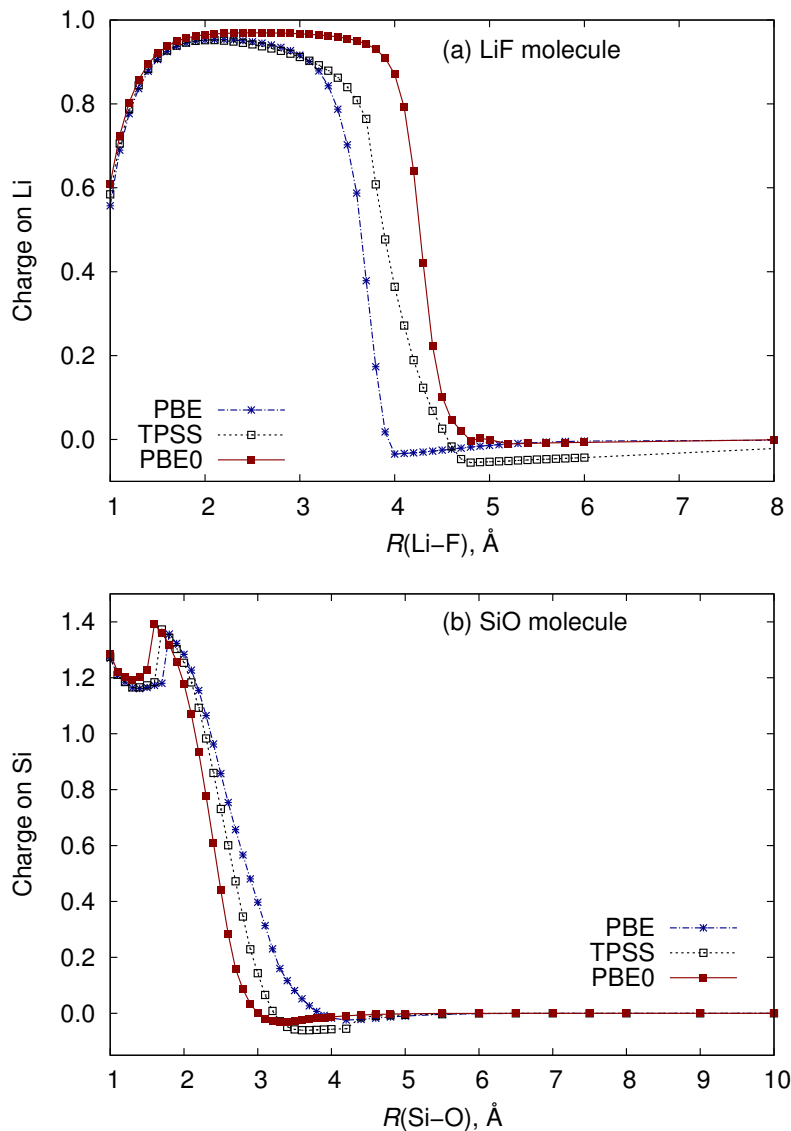
Figure 2.8: Corrected NPA charges on Li in LiF (a) and on Si in SiO (b) versus bond lengths. No residual fractional charges are observed.

2.4 Conclusion

Fractional charges in dissociating polar molecules are a problem of all semilocal DFAs and are a consequence of the many-electron SIE. Within the framework of the method of fractional occupations, the correction is introduced by changing the shape of the exchange-correlation potential of a molecule in such a way that v_{XC} near the less electronegative atom is lowered *relative to* v_{XC} near the more electronegative atom. This is done either by depopulating the HOMO and decreasing the potential in the region where the HOMO is localized or by populating the LUMO and increasing the potential in the

Table 2.2: NPA charges on X (less electronegative atom) at $R = 5 \times R_e$ without fractional occupation and with with a fraction ω of an electron added/removed. ω is determined as described in Section 2.2.3. In polyatomic molecules all the bonds are stretched. The equilibrium bond lengths are from Ref. [24].

XY_n	R_e, Å	PBE			TPSS			PBE0		
		ω	Charge	Corrected charge	ω	Charge	Corrected charge	ω	Charge	Corrected charge
LiF	1.56386	0.686	0.477	−0.001	0.688	0.465	−0.001	0.906	0.420	−0.001
BeO	1.3309	−0.751	0.146	0.000	−0.862	0.108	—[a]	0.000	0.000	0.000
BCl	1.71528	−0.544	0.270	0.000	−0.530	0.246	0.000	−0.597	0.156	0.000
NaCl	2.3608	0.755	0.455	—[a]	0.764	0.466	0.000	0.999	0.433	0.000
NaO	2.05155	0.481	0.299	0.000	0.461	0.275	0.000	0.383	0.151	0.000
MgS[e]	2.1425	0.450	0.148	0.000	0.430	0.134	0.000	0.000	0.000	−0.012
AlO[e]	1.61782	0.421	0.284	0.000	0.373	0.238	0.000	0.246	0.121	0.000
AlC	1.9550[b]	−0.663	0.222	0.000	−0.653	0.190	0.000	−1.000	0.072	0.000
SiO	1.50975	−0.502	0.151	0.000	−0.602	0.195	0.000	0.000	0.000	0.000
CaO[e]	1.8221	0.492	0.315	0.000	0.467	0.298	0.000	0.397	0.179	0.000
GaF	1.77437	0.638	0.441	0.002	0.649	0.422	0.000	0.747	0.366	0.000
GeO	1.62464	−0.546	0.163	0.000	−0.506	0.117	0.000	0.000	0.000	0.000
BeF_2	1.37298[c]	0.999	0.382	0.000	0.999	0.331	0.000	−0.999	0.117	0.000
BF_3	1.313[d]	−0.880	0.547	0.000	−0.921	0.466	0.000	−1.000	0.277	0.000
CO_2[e]	1.160[d]	0.394	0.156	0.004	0.171	0.096	0.000	0.000	0.000	0.000

[a] The calculation could not be converged.
[b] From Ref. [25].
[c] From Ref. [26].
[d] From Ref. [27].
[e] For certain molecules, $\omega < 0$ could not be used with all the three tested functionals, while $\omega > 0$ worked consistently for all of them. In these cases, the choice was made to use the LUMO depopulation throughout.

region where the LUMO is localized. This shift resembles the step structure of the exact exchange-correlation potential. It prevents the electron density from flowing to the more electronegative atom and eliminates partial charges.

The fractional occupation technique is essentially a three-step procedure. Fist, one determines which orbital should be fractionally occupied and what is its optimal occupation number. Next, one performs a self-consistent calculation using the ω determined in the previous step. Finally, the self-consistent orbitals are used in a post-SCF calculation to evaluate the charges. However, the calculation of the optimal value of ω is optional and can be skipped to save computational time. In this work, tuning of ω is mostly done for the purpose of better convergence. If convergence is not an issue, then $\omega \simeq \pm 0.5$ can be used for any molecule.

The correction via the fractional occupation of a FMO not only gives zero charges in the dissociation limit, but also improves the overall behavior of the charges as the molecule is being stretched from its R_e to $R \rightarrow \infty$. Although the experimental critical radii are not reproduced, qualitatively correct sharp decline of the charge is observed.

The method of fractional occupations does not allow one to obtain meaningful energies of dissociating species, therefore, its practical applications are limited. But the significance of this method is that it shows how the step structure of the exact exchange-correlation potential can be mimicked by simply varying the occupation numbers of frontier molecular orbitals.

Bibliography

[1] J. P. Perdew, R. G. Parr, M. Levy, and J. L. Balduz, "Density-functional theory for fractional particle number: Derivative discontinuities of the energy", Phys. Rev. Lett. **49**, 1691–1694 (1982).

[2] A. Ruzsinszky, J. P. Perdew, G. I. Csonka, O. A. Vydrov, and G. E. Scuseria, "Spurious fractional charge on dissociated atoms: Pervasive and resilient self-interaction error of common density functionals", J. Chem. Phys. **125**, 194112 (2006).

[3] A. D. Dutoi and M. Head-Gordon, "Self-interaction error of local density functionals for alkali-halide dissociation", Chem. Phys. Lett. **422**, 230–233 (2006).

[4] O. A. Vydrov, G. E. Scuseria, and J. P. Perdew, "Tests of functionals for systems with fractional electron number", J. Chem. Phys. **126**, 154109 (2007).

[5] J. P. Perdew, A. Ruzsinszky, G. I. Csonka, O. A. Vydrov, G. E. Scuseria, V. N. Staroverov, and J. Tao, "Exchange and correlation in open systems of fluctuating electron number", Phys. Rev. A **76**, 040501 (2007).

[6] A. Makmal, S. Kümmel, and L. Kronik, "Dissociation of diatomic molecules and the exact-exchange Kohn-Sham potential: The case of LiF", Phys. Rev. A **83**, 062512 (2011).

[7] E. Kraisler and L. Kronik, "Elimination of the asymptotic fractional dissociation problem in Kohn-Sham density-functional theory using the ensemble-generalization approach", Phys. Rev. A **91**, 032504 (2015).

[8] J. P. Perdew, K. Burke, and M. Ernzerhof, "Generalized gradient approximation made simple", Phys. Rev. Lett. **77**, Errata: **78**, 1396(E) (1997), 3865–3868 (1996).

[9] J. Tao, J. P. Perdew, V. N. Staroverov, and G. E. Scuseria, "Climbing the density functional ladder: Nonempirical meta-generalized gradient approximation designed for molecules and solids", Phys. Rev. Lett. **91**, 146401 (2003).

[10] C. Adamo and V. Barone, "Toward reliable density functional methods without adjustable parameters: The PBE0 model", J. Chem. Phys. **110**, 6158–6170 (1999).

[11] J. P. Perdew and K. Schmidt, "Jacob's ladder of density functional approximations for the exchange-correlation energy", AIP Conf. Proc. **577**, 1–20 (2001).

[12] O. A. Vydrov and G. E. Scuseria, "Assessment of a long-range corrected hybrid functional", J. Chem. Phys. **125**, 234109 (2006).

[13] B. G. Johnson, P. M. W. Gill, and J. A. Pople, "The performance of a family of density functional methods", J. Chem. Phys. **98**, 5612–5626 (1993).

[14] J. P. Perdew and A. Zunger, "Self-interaction correction to density-functional approximations for many-electron systems", Phys. Rev. B **23**, 5048–5079 (1981).

[15] M. J. Frisch, G. W. Trucks, H. B. Schlegel, G. E. Scuseria, M. A. Robb, J. R. Cheeseman, J. A. Montgomery Jr., T. Vreven, K. N. Kudin, J. C. Burant, J. M. Millam, S. S. Iyengar, J. Tomasi, V. Barone, B. Mennucci, M. Cossi, G. Scalmani, N. Rega, G. A. Petersson, H. Nakatsuji, M. Hada, M. Ehara, K. Toyota, R. Fukuda, J. Hasegawa, M. Ishida, T. Nakajima, Y. Honda, O. Kitao, H. Nakai, M. Klene, X. Li, J. E. Knox, H. P. Hratchian, J. B. Cross, V. Bakken, C. Adamo, J. Jaramillo, R. Gomperts, R. E. Stratmann, O. Yazyev, A. J. Austin, R. Cammi, C. Pomelli, J. W. Ochterski, P. Y. Ayala, K. Morokuma, G. A. Voth, P. Salvador, J. J. Dannenberg, V. G. Zakrzewski, S. Dapprich, A. D. Daniels, M. C. Strain, O. Farkas, D. K. Malick, A. D. Rabuck, K. Raghavachari, J. B. Foresman, J. V. Ortiz, Q. Cui, A. G. Baboul, S. Clifford, J. Cioslowski, B. B. Stefanov, G. Liu, A. Liashenko, P. Piskorz, I. Komaromi, R. L. Martin, D. J. Fox, T. Keith, M. A. Al-Laham, C. Y. Peng, A. Nanayakkara, M. Challacombe, P. M. W. Gill, B. Johnson, W. Chen, M. W. Wong, C. Gonzalez, and J. A. Pople, *Gaussian 03, Revision B.01*, Gaussian Inc., Wallingford, CT, 2004.

[16] M. J. Frisch, G. W. Trucks, H. B. Schlegel, G. E. Scuseria, M. A. Robb, J. R. Cheeseman, G. Scalmani, V. Barone, B. Mennucci, G. A. Petersson, H. Nakatsuji, M. Caricato, X. Li, H. P. Hratchian, A. F. Izmaylov, J. Bloino, G. Zheng, J. L. Sonnenberg, M. Hada, M. Ehara, K. Toyota, R. Fukuda, J. Hasegawa, M. Ishida, T. Nakajima, Y. Honda, O. Kitao, H. Nakai, T. Vreven, J. A. Montgomery Jr., J. E. Peralta, F. Ogliaro, M. Bearpark, J. J. Heyd, E. Brothers, K. N. Kudin, V. N. Staroverov, R. Kobayashi, J. Normand, K. Raghavachari, A. Rendell, J. C. Burant, S. S. Iyengar, J. Tomasi, M. Cossi, N. Rega, J. M. Millam, M. Klene, J. E. Knox, J. B. Cross, V. Bakken, C. Adamo, J. Jaramillo, R. Gomperts, R. E. Stratmann, O. Yazyev, A. J. Austin, R. Cammi, C. Pomelli, J. W. Ochterski, R. L. Martin, K. Morokuma, V. G. Zakrzewski, G. A. Voth, P. Salvador, J. J. Dannenberg, S.

Dapprich, A. D. Daniels,. Farkas, J. B. Foresman, J. V. Ortiz, J. Cioslowski, and D. J. Fox, *Gaussian 09, Revision D.01*, Gaussian Inc., Wallingford, CT 2009.

[17] A. E. Reed, R. B. Weinstock, and F. Weinhold, "Natural population analysis", J. Chem. Phys. **83**, 735–746 (1985).

[18] A. P. Gaiduk, D. S. Firaha, and V. N. Staroverov, "Improved electronic excitation energies from shape-corrected semilocal Kohn-Sham potentials", Phys. Rev. Lett. **108**, 253005 (2012).

[19] A. P. Gaiduk, D. Mizzi, and V. N. Staroverov, "Self-interaction correction scheme for approximate Kohn-Sham potentials", Phys. Rev. A **86**, 052518 (2012).

[20] O. V. Gritsenko and E. J. Baerends, "Effect of molecular dissociation on the exchange-correlation Kohn-Sham potential", Phys. Rev. A **54**, 1957–1972 (1996).

[21] D. G. Tempel, T. J. Martínez, and N. T. Maitra, "Revisiting molecular dissociation in density functional theory: A simple model", J. Chem. Theory Comput. **5**, 770–780 (2009).

[22] S. V. Kohut, A. M. Polgar, and V. N. Staroverov, "Origin of the step structure of molecular exchange-correlation potentials", Phys. Chem. Chem. Phys. **18**, 20938–20944 (2016).

[23] A. P. Gaiduk and V. N. Staroverov, "Construction of integrable model Kohn-Sham potentials by analysis of the structure of functional derivatives", Phys. Rev. A **83**, 012509 (2011).

[24] W. Haynes, *CRC Handbook of Chemistry and Physics, 95th ed.* Internet version, 2015.

[25] C. R. Brazier, "First gas phase spectrum of the aluminum carbide molecule: The $B^4\Sigma^- - X^4\Sigma^-$ system", J. Chem. Phys. **98**, 2790 (1993).

[26] S. Yu, A. Shayesteh, P. F. Bernath, and J. Koput, "The vibration-rotation emission spectrum of hot BeF_2", J. Chem. Phys. **123**, 134303 (2005).

[27] *NIST Computational Chemistry Comparison and Benchmark Database, NIST Standard Reference Database Number 101, Release 17b*, edited by R. D. Johnson III, 2015.

Chapter 3

Excitation energies from Kohn-Sham potentials corrected via addition of fractional nuclear charge

3.1 Introduction

The success of DFT for ground states of molecules encouraged researchers to explore the possibility of applying DFT to excited states. Runge and Gross proved that for a given initial wavefunction, there exists a one-to-one correspondence between the time-dependent density and the time-dependent external potential [1]. The Runge-Gross theorem provides the formal foundation for time-dependent density functional theory (TDDFT) [2, 3]. One can apply the Kohn-Sham approach to an excited state and reduce the interacting many-electron time-dependent problem to a set of one-electron time-dependent Kohn-Sham equations. Just like in the ground-state DFT, the exchange-correlation potential has to be approximated. The most common approximation is the adiabatic approximation, according to which the time-dependent exchange-correlation potential $v_{\mathrm{XC}}([\rho]; \mathbf{r}, t)$ is assumed to react instantaneously to changes in the density with time. In that case, the time-dependent $v_{\mathrm{XC}}([\rho]; \mathbf{r}, t)$ at a moment t in time is just the ground-state $v_{\mathrm{XC}}([\rho]; \mathbf{r})$ which corresponds to the density at time t [4]. A further simplification is to keep only the first-order term in the function that describes system's response to a field. This simplification, called the linear-response regime, is appropriate for weak optical fields usually encountered when calculating electron absorption spectra.

Adiabatic linear-response TDDFT gained popularity as a tool for the calculation of excited states mainly due to its simplicity and applicability for large systems out of

reach for more accurate but computationally demanding wavefunction theories. However, its accuracy is not always satisfactory. The problem is illustrated in Fig. 3.1: the six calculated Rydberg excitation energies of the Mg atom are underestimated. A Rydberg state of an atom arises from the excitation of a valence electron to an orbital with principal quantum number greater than that of any occupied orbital of the ground state (a Rydberg orbital). A molecular Rydberg excitation is an electronic transition into a virtual molecular orbital composed primarily of atomic Rydberg orbitals. If the principal quantum number of an excited orbital is equal to the highest one among the ground-state orbitals, the excited state is called valence. Thus, Rydberg states usually lie higher than valence states. TDDFT gives reasonable accuracy for valence excitations, but it systematically and significantly underestimates Rydberg excitation energies [5–7].
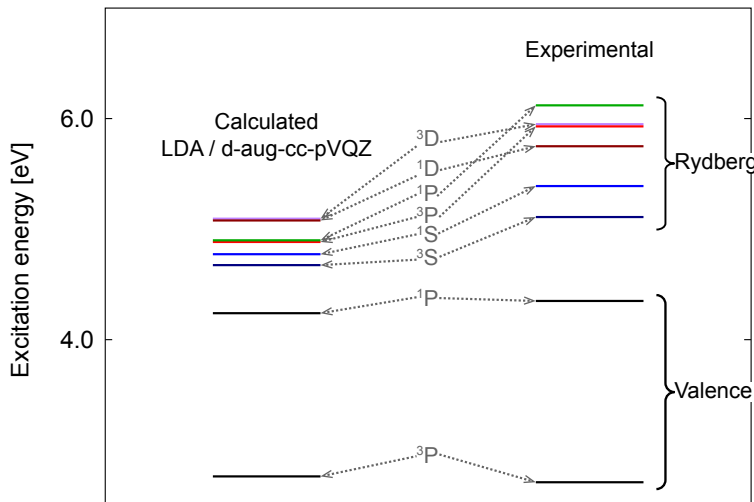

Figure 3.1: Vertical excitation energies of the first 8 excited states of the Mg atom calculated by TDDFT using the LDA functional compared to the corresponding experimental data.

The failures of TDDFT are closely related to the problems of the employed density functionals and, thus, originate from time-independent DFT. In particular, underestimation of the energies of Rydberg states is due to incorrect asymptotic and intermediate range shape of the exchange-correlation potentials derived from semilocal functionals [8–10]. While the exact exchange-correlation potential decays asymptotically as $-1/r$, semilocal exchange-correlation potentials fall off exponentially [11]. As a result, the energy of the highest occupied molecular orbital (HOMO) is insufficiently negative compared to its exact energy, which is equal to the negative of the ionization potential, $\epsilon_{\text{HOMO}}^{\text{exact}} = -I$, and the energies of the high-lying (Rydberg) orbitals are too low. Thus,

the energies of Rydberg excitations are underestimated. Exchange-correlation potentials derived from hybrid density functionals decay asymptotically as $-a/r$ (where a is a constant other than 1) [8], which is closer to the correct $-1/r$ behavior. The underestimation of high-lying excitation energies by hybrid functionals is less pronounced, but still present [12–14].

Numerous attempts have been made to correct long-range behavior of potentials in DFT. These include construction of model exchange-correlation potentials [15–21], inclusion of full exact exchange [22], and use of range-separated hybrids, in which the amount of exact exchange is a function of position in space [23–26].

Improved asymptotic shape of semilocal exchange-correlation potentials can also be achieved via the method of fractional depopulation of the HOMO, developed by Gaiduk *et al.* [27, 28]. In this method, one constructs a model exchange-correlation potential for an N-electron system according to the following equation:

$$v_{\text{XC}}^{\text{corrected}}([\rho]; \mathbf{r}) = v_{\text{HXC}}([\tilde{\rho}]; \mathbf{r}) - v_{\text{H}}([\rho]; \mathbf{r}), \qquad (3.1)$$

where $v_{\text{HXC}}([\tilde{\rho}]; \mathbf{r})$ is the Hartree-exchange-correlation potential of the $(N - \delta)$-electron system with the density $\tilde{\rho}(\mathbf{r})$ obtained by removing a fraction δ of an electron from the HOMO.

The potential corrected in this manner is closer to $-1/r$ in the valence and asymptotic regions than the original potential (Fig. 3.2). In essence, the HOMO depopulation creates a layer of positive charge distributed over the valence region of the atom or molecule. As the amount of an electron removed increases, orbital eigenvalues decrease nearly linearly with larger slopes for valence orbitals than for Rydberg ones. The valence orbital eigenvalues become exact near $\delta = 0.5$, while the Rydberg orbital eigenvalues become exact at larger values of δ. However, the focus of our attention are eigenvalue differences, since they approximate excitation energies [29]. The eigenvalue differences, which are initially underestimated, also increase with δ (Fig. 3.3).

The optimal fraction of an electron to be removed can be adjusted to minimize the mean absolute errors of excitation energies. This parameter has very little system dependence, therefore, it is sufficient to optimize δ for each particular density functional. The HOMO depopulation method can be used with any density functional, it has no added computational cost and is very easy to implement.

Despite its simplicity, the method of the HOMO depopulation significantly improves Rydberg excitation energies, while decent accuracy of valence excitation energies is preserved. In a recent study by Truhlar and co-workers [30], the HOMO depopulation
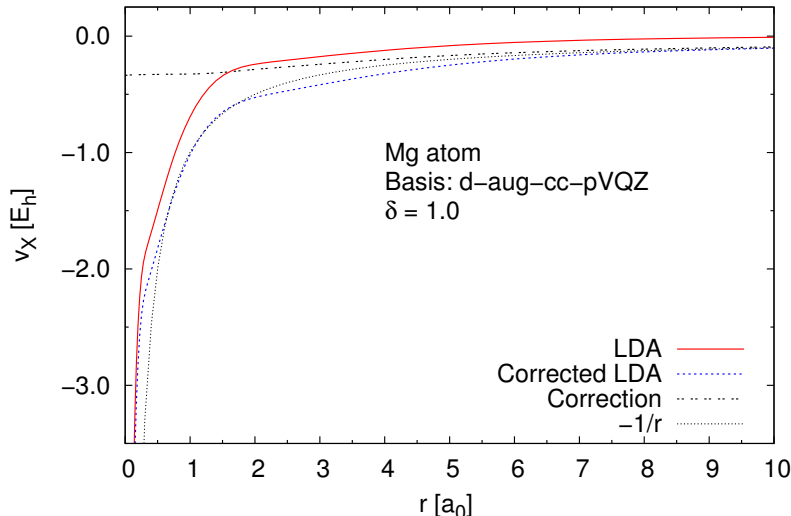
Figure 3.2: LDA exchange potential for the Mg atom without and with correction via the depopulation of the HOMO by one electron. The correction makes v_X^{LDA} closer to $-1/r$ at large and intermediate r.

technique was compared to other methods that predict accurate excitation energies. It was shown on a test set of 69 excited states (both valence and Rydberg) of 11 closed-shell organic molecules that the HOMO depopulation method employing B3LYP (the Becke three parameter hybrid functional [31] with the Lee-Yang-Parr correlation term [32]), BLYP (the Becke-Lee-Yang-Parr generalized gradient approximation) [32, 33], and M06 (the meta generalized gradient hybrid functional of Zhao and Truhlar) [34] outperform equation-of-motion coupled cluster singles and doubles (EOM-CCSD) [35], an accurate and computationally demanding wavefunction-based method.

The HOMO depopulation is not the only way to obtain a fractionally charged system. Another route is to keep the number of electrons in the system integral, but add a fraction of nuclear charge. This should also result in stronger electrostatic interaction between an excited electron and the rest of the system and increase Rydberg excitation energies. Here we investigate whether modification of the nuclear charge may lead to the same improvements in excitation energies as the HOMO depopulation.

3.2   Theory

Recall that in the Kohn-Sham density functional theory [36] the electron density $\rho(\mathbf{r})$ is expressed in terms of Kohn-Sham orbitals, $\rho(\mathbf{r}) = \sum_i^N |\phi_i(\mathbf{r})|^2$. The orbitals are self-
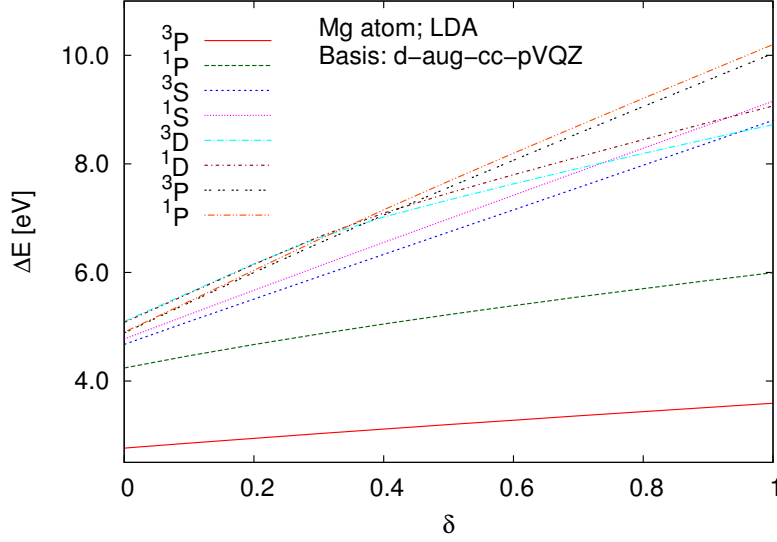
Figure 3.3: Vertical excitation energies of the first 8 excited states of the Mg atom as functions of the fraction of an electron removed from the HOMO.

consistent solutions of the time-independent integro-differential Kohn-Sham equations:

$$\left[-\frac{1}{2}\nabla^2 + v(\mathbf{r}) + v_{\mathrm{HXC}}([\rho]; \mathbf{r})\right] \phi_i(\mathbf{r}) = \epsilon_i \phi_i(\mathbf{r}), \tag{3.2}$$

where $v(\mathbf{r}) = \sum_{A=1}^{M} Z_A/|\mathbf{r} - \mathbf{R}_A|$ is the external potential due to the nuclei, and $v_{\mathrm{HXC}}([\rho]; \mathbf{r})$ is the sum of the Hartree potential $v_{\mathrm{H}}([\rho]; \mathbf{r}) = \int d\mathbf{r}' \rho(\mathbf{r}')/|\mathbf{r} - \mathbf{r}'|$ and the exchange-correlation potential $v_{\mathrm{XC}}([\rho]; \mathbf{r})$, which represents the rest of electron-electron interactions.

Our goal is to test if addition of fractional nuclear charge corrects the shape of the exchange-correlation potential and Rydberg excitation energies in the same manner as the fractional HOMO depopulation does. In order to do so, we use the Kohn-Sham potential of the system with a positive fraction $0 < \zeta \leq 1$ of charge added to the nucleus or distributed among the nuclei (with the weights proportional to their atomic numbers). In this system, the external electrostatic potential due to the nuclei, $v(\mathbf{r})$, is more negative than in the initial system. Clearly, the distribution of the electron density in this system, $\widetilde{\rho}(\mathbf{r})$, is also different from the initial one, $\rho(\mathbf{r})$, with the maximum located closer to the nucleus and lower electron density at intermediate and large distances from the nucleus. Thus, to proceed with construction of the corrected exchange-correlation potential, $v_{\mathrm{XC}}^{\mathrm{corrected}}([\rho]; \mathbf{r})]$, one needs both the Hartree-exchange-correlation and the external potential of the fractionally charged system, which are related to the corresponding

43

potentials of the initial system via the following equation:

$$v(\mathbf{r}) + v_{\mathrm{H}}([\rho]; \mathbf{r}) + v_{\mathrm{XC}}^{\mathrm{corrected}}([\rho]; \mathbf{r})$$
$$= \widetilde{v}(\mathbf{r}) + v_{\mathrm{H}}([\widetilde{\rho}]; \mathbf{r}) + v_{\mathrm{XC}}([\widetilde{\rho}]; \mathbf{r}), \tag{3.3}$$

from which

$$v_{\mathrm{XC}}^{\mathrm{corrected}}([\rho]; \mathbf{r}) = [\widetilde{v}(\mathbf{r}) - v(\mathbf{r})]$$
$$+ [v_{\mathrm{H}}([\widetilde{\rho}]; \mathbf{r}) - v_{\mathrm{H}}([\rho]; \mathbf{r})] + v_{\mathrm{XC}}([\widetilde{\rho}]; \mathbf{r}). \tag{3.4}$$
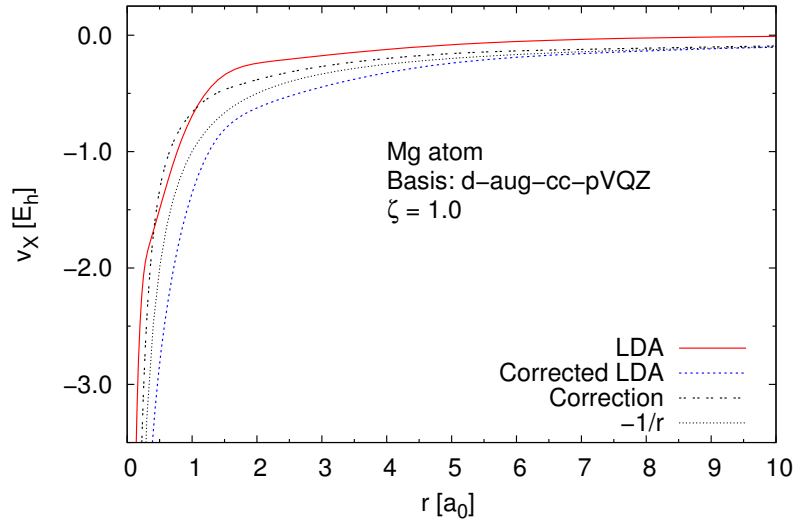

Figure 3.4: LDA exchange potential for the Mg atom without and with correction. The corrected potential is constructed via Eq. 3.4 by adding a unit of nuclear charge ($\zeta = 1.0$). The shape of the corrected LDA exchange potential at large and intermediate r is closer to $-1/r$ than the shape of original LDA exchange potential.

The resulting model exchange-correlation potential is less repulsive and closer to the correct $-1/r$ asymptotic limit, as shown in Fig. 3.4 for the Mg atom. However, the intervention in the nature of the nuclei is not without consequences, and the model potential now has a spurious discontinuity at the nucleus. Despite the presence of this artificial discontinuity, the improved asymptotic behavior should still advance the accuracy of Rydberg excitation energies.

3.3 Methodology

We used the Gaussian 09 program [37] to perform all calculations. The UltraFine integration grid was employed throughout, the basis sets in use were d-aug-cc-pVQZ for atoms and d-aug-cc-pVTZ for molecules. These basis sets were obtained by augmenting the standard aug-cc-pVQZ and aug-cc-pVTZ basis sets with one additional set of diffuse functions of each type (s, p, d, and so on).

The correction procedure can be viewed as a two-step process. First, a self-consistent field (SCF) solution of Kohn-Sham equations is obtained for a chosen density functional and a given system with a fraction of positive charge ζ added to it. An optimal amount of charge ζ to be added was determined by fitting to 14 experimental excitation energies (both valence and Rydberg) of the CO molecule. The value of ζ is slightly different for each functional, but the variation is small. In an atom ζ was placed directly in the centre of the nucleus, and in a molecule it was distributed among all the nuclei with the weights proportional to their atomic numbers. The addition of charge does not require modification of any subroutines as it can be done with the ZNuc keyword in the geometry specification section.

Once the SCF solution is obtained, the self-consistent Kohn-Sham orbitals from the first step are fed to the linear response TDDFT subroutine.

3.4 Results

Addition of fractional nuclear charge makes the HOMO of a molecule more negative (Fig. 3.5), in a manner similar to how it is done via the fractional HOMO depopulation. Energies of the virtual orbitals also decrease, but the higher the orbital energy is, the less it changes with ζ. Thus, the eigenvalue spectrum diverges, and, as a result, energy differences for high-lying virtual orbitals become more pronounced. Since excitation energies can be approximated by Kohn-Sham eigenvalue differences [38], one can expect that addition of fractional nuclear charge will raise excitation energies for high-lying states the most. This is exactly what is necessary in order to correct Rydberg transition energies and keep the already good accuracy of TDDFT for valence excitations, which are typically low-lying.

Addition of fractional nuclear charge leads to an increase of Rydberg excitation energies, which is similar to the effect of the HOMO depopulation. Therefore, the mean absolute error decreases as a function of ζ (Fig. 3.6 for the CO molecule) and reaches a minimum at an optimal value of ζ. As ζ increases further, Rydberg excitation energies
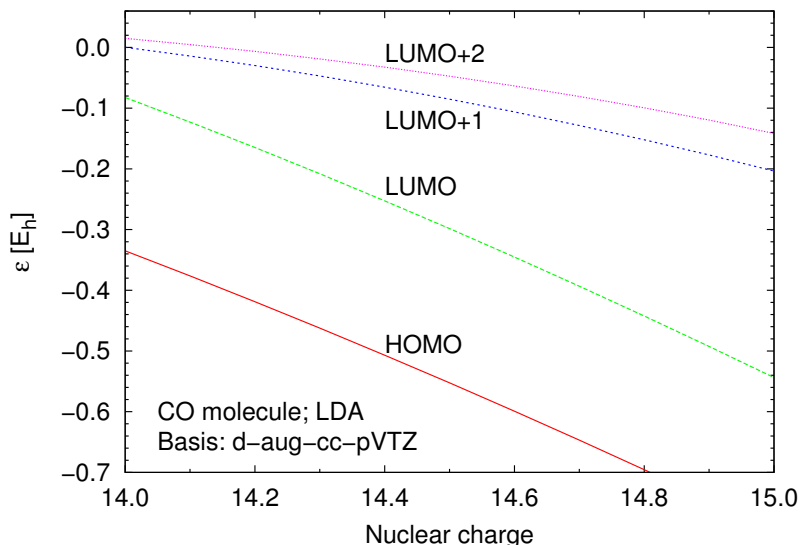
Figure 3.5: LDA orbital eigenvalues in the CO molecule as functions of the fractional nuclear charge. The energies of the virtual orbitals diverge, and while the HOMO-LUMO energy gap does not change significantly, the energy differences for higher lying virtual orbitals increase with nuclear charge.

start to exceed their experimental values and the absolute error increases again. Valence excitation energies, on the other hand, have very little correlation with the amount of added charge. Thus, an optimal ζ allows to obtain an overall improvement of accuracy of excitation energies.

To compare the method of nuclear charge addition to the fractional HOMO depopulation, we computed mean absolute errors of 104 excitation energies, both valence and Rydberg, of three atoms (Be, Mg, Zn) and six molecules (CO, CH_2O, C_2H_2, C_2H_4, H_2O, N_2) at their experimental geometries using four functionals from different classes: the local density approximation (LDA) with the Perdew-Wang parametrization for correlation [39], the Becke-Lee-Yang-Parr (BLYP) generalized gradient approximation [32, 33], the Becke three parameter hybrid functional [31] with the Lee-Yang-Parr correlation term (B3LYP), and the Tao-Perdew-Staroverov-Scuseria (TPSS) meta-generalized gradient approximation [40]. The mean absolute errors for the 31 valence and 73 Rydberg excitations of these atoms and molecules are given in Table 3.1, and Fig. 3.7 shows how the correction via the addition of fractional nuclear charge compares to the HOMO depopulation on the example of the BLYP functional.

According to the results presented in Table 3.1 and Fig. 3.7, addition of fractional nuclear charge indeed reduces errors in Rydberg excitations, and in several cases it even outperforms the method of fractional HOMO depopulation. However, while the effect of
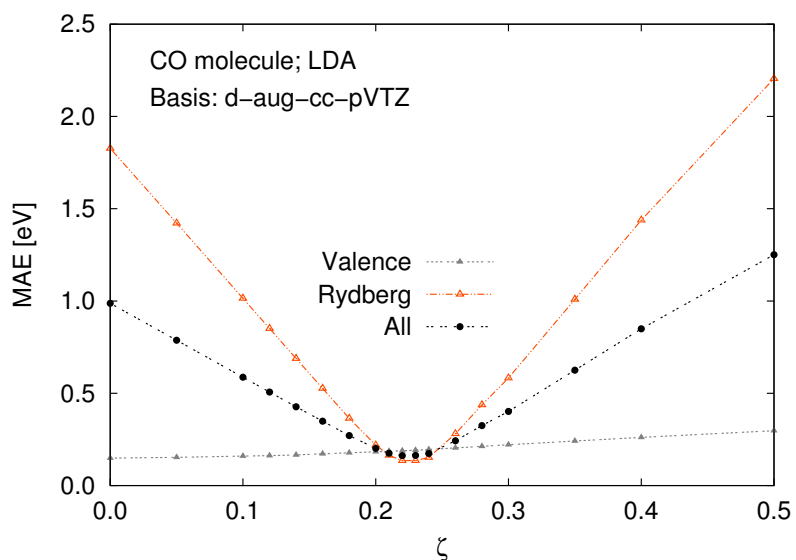
Figure 3.6: Mean absolute error of 7 valence and 7 Rydberg excitation energies of the CO molecule with respect to experimental data as a function of the amount of added nuclear charge, ζ. The minimum on the overall curve corresponds to an optimal value of ζ.

Figure 3.7: Mean absolute errors of 28 excitation energies of atoms and 76 excitation energies of molecules calculated using the BLYP functional without any corrections, with the correction via the addition of fractional nuclear charge, and with the correction via the HOMO depopulation. The HOMO depopulation outperforms the addition of nuclear charge since it works consistently well for both atoms and molecules.

the fractional HOMO depopulation is consistent for both atoms and molecules, and the mean absolute errors are reduced to 0.2 eV, the addition of fractional nuclear charge does not work as well for atoms as it does for molecules. This makes the overall performance of the nuclear charge addition method worse than that of the fractional HOMO depopulation, with the mean absolute error of about 0.3 eV. A closer look at the improved excitation energies of atoms (Tables 3.2–3.4) shows that the new correction method overestimates, or overcorrects them. Thus, the optimal values of ζ found by fitting to 14 experimental excitation energies of the CO molecule turn out to be non-optimal for atoms.
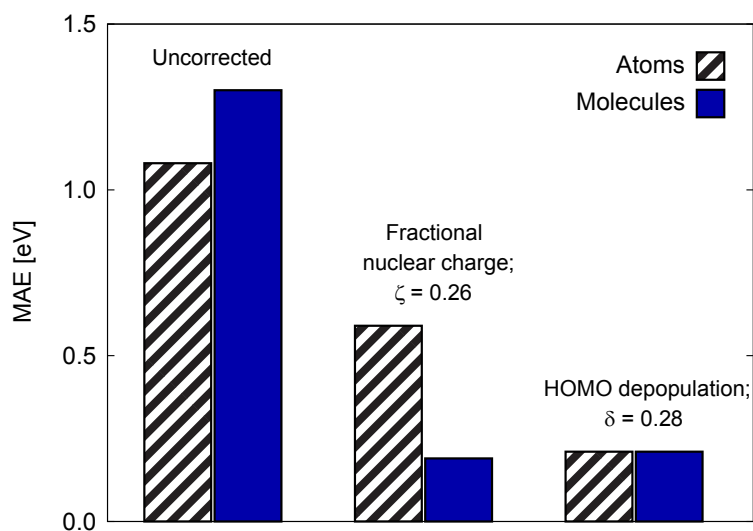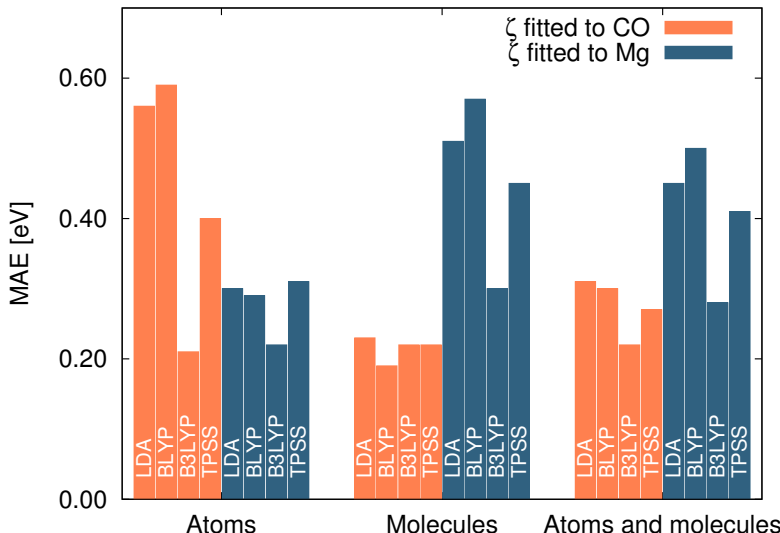

Figure 3.8: Mean absolute errors of 28 excitation energies of atoms and 76 excitation energies of molecules calculated using two different sets of added charges ζ: one set was fitted to 14 experimental excitation energies of the CO molecule, and the other set was fitted to 8 experimental excitation energies of the Mg atom. The latter set gives better results for atoms but fails for molecules.

To find out whether a different choice of optimal ζ values can lead to better results, we determined a new set of ζ's by fitting 8 calculated excitation energies of the Mg atom to experimental data. This gave lower values: $\zeta = 0.11$ for LDA and B3LYP, $\zeta = 0.15$ for BLYP, and $\zeta = 0.13$ for TPSS. Although these parameters were indeed optimal for atoms, and lowered the mean absolute errors of the excitation energies of atoms to 0.30, 0.29, 0.22, and 0.31 eV for LDA, BLYP, B3LYP, and TPSS respectively (Table 3.1), the errors in excitation energies of molecules increased (Fig. 3.8), leading to a worse overall performance with the errors for atoms and molecules of 0.45, 0.50, 0.28, and 0.41 eV.

In principle, one could solve the problem by using different optimal ζ values for

Table 3.1: Mean absolute errors in eV of 104 vertical excitation energies of three atoms (Be, Mg, Zn) and six molecules (CO, CH$_2$O, C$_2$H$_2$, C$_2$H$_4$, H$_2$O, N$_2$) calculated using TDDFT, with respect to experimental values. Basis sets are d-aug-cc-pVQZ for atoms and d-aug-cc-pVTZ for molecules. The results of correction by the HOMO depopulation method are compared to the effect of nuclear charge addition.

Potentials	Atoms			Molecules			Atoms and molecules		
	Valence	Rydberg	All	Valence	Rydberg	All	Valence	Rydberg	All
Uncorrected									
LDA	0.22	1.01	0.84	0.27	1.39	1.02	0.26	1.27	0.97
BLYP	0.29	1.29	1.08	0.35	1.77	1.30	0.34	1.62	1.24
B3LYP	0.29	0.96	0.81	0.36	0.98	0.78	0.35	0.97	0.79
TPSS	0.49	1.12	0.99	0.31	1.45	1.08	0.34	1.35	1.05
HOMO depopulation									
LDA ($\delta = 0.24$)	0.29	0.23	0.24	0.22	0.25	0.24	0.23	0.24	0.24
BLYP ($\delta = 0.28$)	0.32	0.18	0.21	0.26	0.18	0.21	0.28	0.18	0.21
B3LYP ($\delta = 0.18$)	0.24	0.29	0.28	0.38	0.15	0.23	0.36	0.19	0.24
TPSS ($\delta = 0.23$)	0.35	0.22	0.25	0.29	0.19	0.22	0.30	0.19	0.23
Addition of nuclear charge:									
ζ fitted to CO									
LDA ($\zeta = 0.22$)	0.48	0.58	0.56	0.24	0.22	0.23	0.29	0.33	0.31
BLYP ($\zeta = 0.26$)	0.56	0.59	0.59	0.25	0.16	0.19	0.31	0.29	0.30
B3LYP ($\zeta = 0.14$)	0.24	0.21	0.21	0.34	0.17	0.22	0.32	0.18	0.22
TPSS ($\zeta = 0.20$)	0.42	0.40	0.40	0.31	0.18	0.22	0.33	0.24	0.27
ζ fitted to Mg									
LDA ($\zeta = 0.11$)	0.22	0.32	0.30	0.26	0.63	0.51	0.25	0.54	0.45
BLYP ($\zeta = 0.15$)	0.31	0.28	0.29	0.27	0.72	0.57	0.28	0.59	0.50
B3LYP ($\zeta = 0.11$)	0.17	0.23	0.22	0.33	0.29	0.30	0.30	0.27	0.28
TPSS ($\zeta = 0.13$)	0.35	0.30	0.31	0.30	0.53	0.45	0.31	0.46	0.41

atoms than for molecules. However, this means that the correction by the addition of fractional nuclear charge lacks one major advantage of the fractional HOMO depopulation technique—system independence of parameter ζ.

3.5   Conclusion

We tested whether fractionally charged systems with partial nuclear charges and integral numbers of electrons are as efficient for improving excitation energies as systems with integral nuclear charges and fractionally depopulated HOMOs. In both approaches, the model potentials are less repulsive, which allows one to obtain corrected (more negative) HOMO eigenvalues as well as larger orbital energy differences and higher vertical excitation energies.

Since excitation energies increase linearly with the amount of nuclear charge added, ζ, using high values of ζ leads to an overestimation of excitation energies. The optimal values of ζ are different (but not significantly) for different density functionals and can be determined by fitting to experimental excitation energies of an atom or a molecule.

Similarly to the HOMO depopulation, the approach of fractional nuclear charge addition can be applied to any density functional and does not require additional computational time. It is also simpler than the fractional HOMO depopulation method in terms of implementation.

However, the optimal amount of added nuclear charge for atoms appears to be significantly different from the optimal amount of added charge for molecules (0.1 versus 0.2). Consequently, the overall reduction of the mean absolute errors of excitation energies in a test set consisting of both atoms and molecules is not as notable as with the method of fractional HOMO occupations. Because of system dependence of parameter ζ, the fractional nuclear charge approach is less favourable than the fractional HOMO depopulation technique.

Table 3.2: Valence and Rydberg excitation energies (in eV) for the Be atom calculated by TDDFT using various density functionals with and without the correction by adding a fraction of nuclear charge ζ.

Be	Uncorrected potentials				Corrected potentials								
	LDA	BLYP	B3LYP	TPSS	LDA		BLYP		B3LYP		TPSS		Expt.[a]
State Transition	$\zeta = 0$				$\zeta = 0.11$	$\zeta = 0.22$	$\zeta = 0.15$	$\zeta = 0.26$	$\zeta = 0.11$	$\zeta = 0.14$	$\zeta = 0.13$	$\zeta = 0.20$	
^3P $2s \rightarrow 2p$	2.40	2.09	2.09	1.58	2.59	2.77	2.28	2.42	2.24	2.27	1.78	1.88	2.73
^1P $2s \rightarrow 2p$	4.85	4.85	4.89	5.05	5.30	5.72	5.47	5.90	5.33	5.44	5.60	5.89	5.28
^3S $2s \rightarrow 3s$	5.51	5.29	5.62	5.62	6.37	7.27	6.52	7.42	6.49	6.73	6.67	7.25	6.46
^1S $2s \rightarrow 3s$	5.62	5.40	5.80	5.75	6.53	7.47	6.71	7.66	6.73	6.98	6.86	7.45	6.78
^3P $2s \rightarrow 3p$	5.66	5.51	6.05	5.80	6.72	7.79	6.94	7.98	7.07	7.34	7.07	7.74	7.30
^1P $2s \rightarrow 3p$	5.66	5.52	6.13	5.80	6.73	7.83	6.98	8.06	7.16	7.43	7.09	7.81	7.46
^3D $2s \rightarrow 3d$	6.61	6.33	6.68	6.67	7.51	8.48	7.61	8.60	7.63	7.89	7.77	8.39	7.69
^1D $2s \rightarrow 3d$	6.52	6.28	6.62	6.66	7.43	8.40	7.57	8.57	7.58	7.84	7.77	8.39	7.99
Mean absolute errors with respect to experiment													
Valence (2)	0.37	0.53	0.51	0.68	0.08	0.24	0.32	0.46	0.27	0.31	0.64	0.73	
Rydberg (6)	1.35	1.56	1.13	1.23	0.40	0.59	0.24	0.77	0.18	0.15	0.20	0.56	
All (8)	1.11	1.30	0.97	1.09	0.32	0.51	0.26	0.69	0.20	0.19	0.31	0.60	

[a]From Ref. [41].

Table 3.3: Valence and Rydberg excitation energies (in eV) for the Mg atom calculated by TDDFT using various density functionals with and without the correction by adding a fraction of nuclear charge ζ.

Mg	Uncorrected potentials				Corrected potentials								
	LDA	BLYP	B3LYP	TPSS	LDA		BLYP		B3LYP		TPSS		Expt.[a]
State Transition	$\zeta = 0$				$\zeta = 0.11$	$\zeta = 0.22$	$\zeta = 0.15$	$\zeta = 0.26$	$\zeta = 0.11$	$\zeta = 0.14$	$\zeta = 0.13$	$\zeta = 0.20$	
^3P $3s \to 3p$	2.76	2.66	2.61	2.16	2.98	3.20	2.94	3.15	2.82	2.87	2.38	2.50	2.71
^1P $3s \to 3p$	4.24	4.15	4.23	4.18	4.65	5.05	4.75	5.16	4.64	4.74	4.64	4.88	4.35
^3S $3s \to 4s$	4.67	4.40	4.66	4.63	5.31	5.96	5.33	5.99	5.31	5.47	5.38	5.80	5.11
^1S $3s \to 4s$	4.77	4.49	4.80	4.73	5.44	6.12	5.49	6.18	5.50	5.67	5.52	5.95	5.39
^3D $3s \to 3d$	5.10	4.78	5.23	5.05	5.85	6.64	5.76	6.62	5.94	6.18	5.94	6.44	5.95
^1D $3s \to 3d$	5.08	4.78	5.22	5.05	5.84	6.63	5.75	6.62	5.93	6.18	5.95	6.45	5.75
^3P $3s \to 4p$	4.88	4.62	5.06	4.84	5.67	6.47	5.67	6.50	5.84	6.05	5.75	6.25	5.93
^1P $3s \to 4p$	4.90	4.66	5.13	4.87	5.68	6.51	5.69	6.55	5.91	6.14	5.80	6.32	6.12
Mean absolute errors with respect to experiment													
Valence (2)	0.08	0.12	0.11	0.36	0.29	0.60	0.32	0.62	0.20	0.28	0.31	0.37	
Rydberg (6)	0.81	1.09	0.69	0.85	0.19	0.68	0.20	0.70	0.13	0.24	0.18	0.49	
All (8)	0.63	0.85	0.55	0.72	0.21	0.66	0.23	0.68	0.15	0.25	0.21	0.46	

[a]From Ref. [41].

Table 3.4: Valence and Rydberg excitation energies (in eV) for the Zn atom calculated by TDDFT using various density functionals with and without the correction by adding a fraction of nuclear charge ζ.

Zn

| | Uncorrected potentials | | | | Corrected potentials | | | | | | | | |
| | $\zeta = 0$ | | | | LDA | | BLYP | | B3LYP | | TPSS | | |
State Transition	LDA	BLYP	B3LYP	TPSS	$\zeta=0.11$	$\zeta=0.22$	$\zeta=0.15$	$\zeta=0.26$	$\zeta=0.11$	$\zeta=0.14$	$\zeta=0.13$	$\zeta=0.20$	Expt.[a]
^3P $4s \to 4p$	4.19	4.07	3.89	3.62	4.42	4.64	4.38	4.60	4.11	4.17	3.87	4.00	4.03
^1P $4s \to 4p$	5.58	5.42	5.42	5.35	5.99	6.38	6.02	6.41	5.82	5.93	5.82	6.06	5.80
^3S $4s \to 5s$	6.05	5.68	5.90	5.72	6.73	7.42	6.66	7.33	6.59	6.76	6.56	6.94	6.65
^1S $4s \to 5s$	6.11	5.76	6.02	5.83	6.82	7.54	6.79	7.49	6.75	6.93	6.67	7.11	6.92
^3P $4s \to 5p$	6.35	5.98	6.35	6.06	7.14	7.95	7.09	7.90	7.17	7.38	6.98	7.47	7.60
^1P $4s \to 5p$	6.42	6.09	6.45	6.15	7.19	8.00	7.16	7.98	7.26	7.47	7.05	7.56	7.80
^3D $4s \to 4d$	7.47	7.08	7.22	7.09	8.10	8.75	7.94	8.58	7.85	8.02	7.84	8.24	7.78
^1D $4s \to 4d$	7.36	7.02	7.15	7.07	8.00	8.66	7.89	8.55	7.79	7.97	7.82	8.23	7.74
^3S $4s \to 6s$	6.90	6.59	6.86	6.63	7.61	8.37	7.60	8.36	7.64	7.84	7.49	7.94	8.11
^1S $4s \to 6s$	7.04	6.75	7.01	6.78	7.73	8.47	7.71	8.46	7.75	7.95	7.59	8.05	8.19
^3P $4s \to 6p$	7.30	6.95	7.20	6.89	7.98	8.71	7.83	8.57	7.88	8.07	7.79	8.19	8.44
^1P $4s \to 6p$	7.56	7.29	7.48	7.25	8.20	8.89	8.11	8.78	8.11	8.29	8.03	8.43	8.51
Mean absolute errors with respect to experiment													
Valence (2)	0.19	0.21	0.26	0.43	0.29	0.59	0.28	0.59	0.05	0.13	0.09	0.15	
Rydberg (10)	0.92	1.25	1.01	1.23	0.36	0.50	0.36	0.42	0.32	0.22	0.42	0.24	
All (12)	0.80	1.08	0.88	1.09	0.34	0.52	0.35	0.45	0.28	0.21	0.37	0.23	

[a]From Ref. [41].

Table 3.5: Valence and Rydberg excitation energies (in eV) for the CO molecule calculated by TDDFT using various density functionals with and without the correction by adding a fraction of nuclear charge ζ. Molecular geometry: $r(CO) = 1.128$Å.

CO		Uncorrected potentials				Corrected potentials								
		LDA	BLYP	B3LYP	TPSS	LDA		BLYP		B3LYP		TPSS		Expt[a]
State	Transition	$\zeta = 0$	$\zeta = 0$	$\zeta = 0$	$\zeta = 0$	$\zeta = 0.11$	$\zeta = 0.22$	$\zeta = 0.15$	$\zeta = 0.26$	$\zeta = 0.11$	$\zeta = 0.14$	$\zeta = 0.13$	$\zeta = 0.20$	
$^3\Pi$	$\sigma \rightarrow \pi^*$	5.97	5.82	5.86	5.79	5.96	5.94	5.79	5.76	5.83	5.82	5.77	5.75	6.32
$^3\Sigma^+$	$\pi \rightarrow \pi^*$	8.43	8.09	7.95	7.99	8.50	8.55	8.18	8.23	8.02	8.02	8.06	8.09	8.51
$^1\Pi$	$\sigma \rightarrow \pi^*$	8.17	8.23	8.39	8.45	8.27	8.34	8.38	8.45	8.47	8.50	8.58	8.63	8.51
$^3\Delta$	$\pi \rightarrow \pi^*$	9.19	8.68	8.64	8.64	9.28	9.35	8.79	8.85	8.72	8.73	8.73	8.78	9.36
$^3\Sigma^-$	$\pi \rightarrow \pi^*$	9.88	9.77	9.73	10.06	9.98	10.08	9.93	10.02	9.83	9.85	10.10	10.26	9.88
$^1\Sigma^-$	$\pi \rightarrow \pi^*$	9.88	9.77	9.73	10.06	9.98	10.08	9.93	10.02	9.83	9.85	10.20	10.26	9.88
$^1\Delta$	$\pi \rightarrow \pi^*$	10.33	10.01	10.04	10.16	10.45	10.56	10.17	10.27	10.15	10.18	10.31	10.37	10.23
$^3\Sigma^+$	$\sigma \rightarrow 3s\sigma$	9.04	8.74	9.56	9.12	9.82	10.60	9.81	10.57	10.28	10.54	10.08	10.58	10.40
$^1\Sigma^+$	$\sigma \rightarrow 3s\sigma$	9.22	8.94	9.86	9.34	10.05	10.87	10.07	10.88	10.63	10.90	10.35	10.88	10.78
$^3\Sigma^+$	$\sigma \rightarrow 3p\sigma$	9.50	9.21	10.18	9.60	10.42	11.34	10.45	11.38	11.01	11.32	10.71	11.30	11.30
$^1\Sigma^+$	$\sigma \rightarrow 3p\sigma$	9.50	9.22	10.20	9.65	10.43	11.37	10.49	11.45	11.07	11.39	10.76	11.37	11.4
$^3\Pi$	$\pi \rightarrow 3p\pi$	9.52	9.24	10.25	9.63	10.45	11.38	10.52	11.44	11.11	11.41	10.75	11.35	11.55
$^1\Pi$	$\pi \rightarrow 3p\pi$	9.54	9.28	10.29	9.68	10.46	11.39	10.55	11.47	11.15	11.45	10.79	11.40	11.53
$^1\Sigma^+$	$\sigma \rightarrow 3d\sigma$	10.26	9.99	11.04	10.40	11.21	12.12	11.28	12.26	11.92	12.25	11.53	12.14	12.4
		Mean absolute errors with respect to experiment												
Valence (7)		0.15	0.33	0.34	0.32	0.16	0.19	0.24	0.25	0.26	0.25	0.33	0.37	
Rydberg (7)		1.83	2.11	1.14	1.70	0.93	0.14	0.88	0.10	0.31	0.09	0.63	0.13	
All (14)		0.99	1.22	0.74	1.01	0.55	0.16	0.56	0.17	0.29	0.17	0.48	0.25	

[a]From Ref. [42].

Table 3.6: Valence and Rydberg excitation energies (in eV) for the CH$_2$O molecule calculated by TDDFT using various density functionals with and without the correction by adding a fraction of nuclear charge ζ. Molecular geometry: r(CO) = 1.205Å, r(CH) = 1.111Å, θ(HCO) = 121.9°.

CH$_2$O

		Uncorrected potentials				Corrected potentials								
		LDA	BLYP	B3LYP	TPSS	LDA		BLYP		B3LYP		TPSS		Expt.[a]
State	Transition	$\zeta=0$				$\zeta=0.11$	$\zeta=0.22$	$\zeta=0.15$	$\zeta=0.26$	$\zeta=0.11$	$\zeta=0.14$	$\zeta=0.13$	$\zeta=0.20$	
$^3A_2$	$n \to \pi^*$	3.09	3.15	3.22	3.26	3.11	3.13	3.18	3.20	3.25	3.26	3.20	3.31	3.50
$^1A_2$	$n \to \pi^*$	3.70	3.84	3.94	4.06	3.73	3.77	3.90	3.94	3.99	4.00	4.11	4.14	3.94
$^3A_1$	$\pi \to \pi^*$	6.24	5.80	5.46	5.59	6.25	6.26	5.81	5.81	5.45	5.45	5.59	5.59	5.53
$^3B_2$	$n \to 3sa_1$	5.81	5.53	6.32	5.85	6.39	6.93	6.31	6.83	6.88	7.02	6.54	6.90	6.83
$^1B_2$	$n \to 3sa_1$	5.87	5.62	6.44	5.96	6.49	7.09	6.47	7.05	7.06	7.22	6.73	7.12	7.09
$^3A_1$	$n \to 3pb_2$	6.48	6.21	7.13	6.49	7.25	7.95	7.22	7.89	7.83	8.02	7.42	7.88	7.79
$^1A_1$	$n \to 3pb_2$	6.48	6.22	7.18	6.53	7.28	8.03	7.28	8.01	7.93	8.12	7.49	7.98	7.97
$^3B_2$	$n \to 3pa_1$	6.58	6.30	7.12	6.61	7.29	7.93	7.25	7.88	7.77	7.94	7.47	7.90	7.96
$^1B_2$	$n \to 3pa_1$	6.59	6.34	7.20	6.65	7.33	8.01	7.33	8.00	7.89	8.07	7.55	8.00	8.12
$^1B_1$	$\sigma \to \pi^*$	8.76	8.78	9.00	9.01	8.88	8.98	8.95	9.04	9.09	9.12	9.15	9.19	8.68
$^1A_2$	$n \to 3pb_1$	6.69	6.41	7.38	6.73	7.50	8.30	7.51	8.30	8.17	8.38	7.71	8.22	8.37
$^1A_2$	$n \to 3pb_1$	7.53	7.25	8.20	7.56	8.33	9.15	8.36	9.19	9.04	9.27	8.53	9.06	9.22
						Mean absolute errors with respect to experiment								
Valence (4)		0.36	0.21	0.17	0.19	0.38	0.40	0.23	0.23	0.19	0.20	0.25	0.24	
Rydberg (8)		1.41	1.68	0.80	1.37	0.68	0.07	0.70	0.06	0.12	0.10	0.49	0.08	
All (12)		1.06	1.19	0.59	0.98	0.58	0.18	0.54	0.12	0.15	0.14	0.41	0.14	

[a]From Ref. [43].

Table 3.7: Valence and Rydberg excitation energies (in eV) for the C$_2$H$_2$ molecule calculated by TDDFT using various density functionals with and without the correction by adding a fraction of nuclear charge ζ. Molecular geometry: $r(CC) = 1.203$Å, $r(CH) = 1.063$Å.

C$_2$H$_2$

| State Transition | Uncorrected potentials | | | | Corrected potentials | | | | | | | | |
| | LDA | BLYP | B3LYP | TPSS | LDA | | BLYP | | B3LYP | | TPSS | | Expt.[a] |
	$\zeta = 0$				$\zeta=0.11$	$\zeta=0.22$	$\zeta=0.15$	$\zeta=0.26$	$\zeta=0.11$	$\zeta=0.14$	$\zeta=0.13$	$\zeta=0.20$	
$^3\Sigma_u^+$ $\pi_u \rightarrow \pi_g$	5.53	5.22	5.03	4.96	5.56	5.59	5.25	5.26	5.02	5.02	4.96	4.96	5.20
$^3\Delta_u$ $\pi_u \rightarrow \pi_g$	6.21	5.78	5.70	5.77	6.29	6.35	5.86	5.90	5.74	5.75	5.82	5.84	6.00
$^1\Delta_u$ $\pi_u \rightarrow \pi_g$	7.02	6.77	6.80	6.96	6.89	7.30	6.98	7.09	6.92	6.76	7.14	7.21	7.20
$^3\Pi_u$ $\pi_u \rightarrow 3s\sigma_g$	7.16	6.68	7.22	6.98	7.78	8.39	7.52	8.12	7.81	7.97	7.73	8.12	8.07
$^1\Pi_u$ $\pi_u \rightarrow 3s\sigma_g$	7.17	6.71	7.26	7.02	7.81	8.43	7.57	8.18	7.86	8.03	7.78	8.18	8.16
$^3\Pi_g$ $\pi_u \rightarrow 3p\sigma_u$	7.37	6.87	7.43	7.19	7.94	8.41	7.60	8.04	7.92	8.05	7.86	8.16	8.90
$^3\Sigma_g^+$ $\pi_u \rightarrow 3p\pi_u$	7.71	7.23	7.88	7.49	8.43	9.15	8.24	8.94	8.55	8.75	8.35	8.81	8.98
$^1\Pi_g$ $\pi_u \rightarrow 3p\sigma_u$	7.42	6.94	7.55	7.26	8.06	8.62	7.78	8.31	8.12	8.27	8.03	8.40	9.00
$^3\Delta_g$ $\pi_u \rightarrow 3p\pi_u$	7.73	7.25	7.89	7.53	8.46	9.19	8.23	8.94	8.59	8.78	8.39	8.86	9.08
$^3\Pi_u$ $\pi_u \rightarrow 3d\sigma_g$	7.81	7.36	8.15	7.65	8.61	9.32	8.45	9.23	8.79	9.22	8.60	9.14	9.17
$^1\Sigma_g^+$ $\pi_u \rightarrow 3p\pi_u$	7.78	7.31	8.01	7.60	8.53	9.29	8.36	8.95	8.59	8.79	8.50	8.88	9.21
$^1\Pi_u^+$ $\pi_u \rightarrow 3d\sigma_g$	7.82	7.37	8.18	7.67	8.62	9.44	8.48	9.28	8.91	9.23	8.62	9.15	9.24[b]
Mean absolute errors with respect to experiment													
Valence (3)	0.24	0.22	0.29	0.24	0.32	0.28	0.14	0.09	0.24	0.29	0.16	0.14	
Rydberg (9)	1.31	1.79	1.14	1.49	0.62	0.24	0.84	0.24	0.52	0.31	0.66	0.25	
All (12)	1.05	1.40	0.93	1.18	0.54	0.25	0.67	0.20	0.45	0.31	0.54	0.22	

[a] From Ref. [44] (except for the $^1\Pi_u$ state).
[b] From Ref. [45].

56

Table 3.8: Valence and Rydberg excitation energies (in eV) for the C_2H_4 molecule calculated by TDDFT using various density functionals with and without the correction by adding a fraction of nuclear charge ζ. Molecular geometry: $r(CC) = 1.339$Å, $r(CH) = 1.086$Å, $\theta(HCC) = 121.2°$.

C_2H_4

	Uncorrected potentials				Corrected potentials								
	LDA	BLYP	B3LYP	TPSS	LDA	BLYP			B3LYP		TPSS		
	$\zeta = 0$				$\zeta = 0.11$	$\zeta = 0.22$	$\zeta = 0.15$	$\zeta = 0.26$	$\zeta = 0.11$	$\zeta = 0.14$	$\zeta = 0.13$	$\zeta = 0.20$	Expt.[a]
State Transition													
$^3B_{1u}$ $\pi \rightarrow \pi^*(b_{2g})$	4.65	4.27	4.02	4.03	4.65	4.65	4.25	4.24	3.99	3.98	4.00	3.99	4.36
$^3B_{3u}$ $\pi \rightarrow 3s(a_g)$	6.55	6.08	6.49	6.38	7.01	7.45	6.72	7.16	6.94	7.05	6.96	7.25	6.98
$^1B_{3u}$ $\pi \rightarrow 3s(a_g)$	6.59	6.14	6.56	6.44	7.08	7.54	6.81	7.27	7.03	7.16	7.05	7.36	7.11
$^3B_{1g}$ $\pi \rightarrow 3p\sigma(b_{2u})$	6.96	6.54	7.05	6.83	7.03	7.09	7.20	7.29	7.46	7.49	7.43	7.50	7.79
$^1B_{1g}$ $\pi \rightarrow 3p\sigma(b_{2u})$	7.03	6.56	7.08	6.85	7.51	7.59	7.34	7.83	7.60	7.74	7.57	7.92	7.80
$^1B_{2g}$ $\pi \rightarrow 3p\sigma(b_{1u})$	7.02	6.52	7.07	6.82	7.61	8.16	7.31	7.83	7.61	7.76	7.54	7.90	7.90
$^1B_{1u}$ $\pi \rightarrow \pi^*(b_{2g})$	7.35	7.00	7.30	7.26	7.62	7.80	7.49	7.69	7.53	7.58	7.65	7.78	8.00
^3A_g $\pi \rightarrow 3p\pi(b_{3u})$	7.26	6.75	7.30	7.00	7.89	8.51	7.62	8.24	7.91	8.07	7.76	8.15	8.15
^1A_g $\pi \rightarrow 3p\pi(b_{3u})$	7.29	6.79	7.37	7.07	7.93	8.58	7.68	8.32	8.00	8.17	7.85	8.26	8.28
$^3B_{3u}$ $\pi \rightarrow 3d\sigma(a_g)$	7.30	6.85	7.53	7.12	8.00	8.71	7.80	8.50	8.23	8.41	7.96	8.41	8.57
$^1B_{3u}$ $\pi \rightarrow 3d\sigma(a_g)$	7.32	6.87	7.55	7.15	8.02	8.72	7.82	8.53	8.25	8.44	7.98	8.44	8.62
$^1B_{3u}$ $\pi \rightarrow 3d\delta(a_g)$	7.62	7.13	7.77	7.41	8.30	8.99	8.06	8.75	8.45	8.64	8.24	8.68	8.90
$^1B_{2u}$ $\pi \rightarrow 3d\delta(b_{1g})$	8.20	7.70	8.22	8.00	8.81	9.41	8.53	9.15	8.82	8.98	8.73	9.12	9.05
$^1B_{1u}$ $\pi \rightarrow 3d\pi(b_{2g})$	7.80	7.43	7.95	7.68	8.44	9.14	8.21	8.88	8.61	8.80	8.38	8.82	9.33
Mean absolute errors with respect to experiment													
Valence (2)	0.47	0.55	0.52	0.53	0.34	0.24	0.31	0.22	0.42	0.40	0.35	0.30	
Rydberg (12)	0.96	1.43	0.88	1.14	0.41	0.30	0.58	0.16	0.30	0.17	0.42	0.17	
All (14)	0.89	1.30	0.83	1.06	0.40	0.29	0.54	0.17	0.32	0.20	0.41	0.19	

[a]From Ref. [46].

Table 3.9: Rydberg excitation energies (in eV) for the H_2O molecule calculated by TDDFT using various density functionals with and without the correction by adding a fraction of nuclear charge ζ. Molecular geometry: $r(OH) = 0.958$Å, $\theta(HOH) = 104.5°$.

H_2O		Uncorrected potentials				Corrected potentials								
		LDA	BLYP	B3LYP	TPSS	LDA		BLYP		B3LYP		TPSS		Expt.[a]
		$\zeta = 0$				$\zeta = 0.11$	$\zeta = 0.22$	$\zeta = 0.15$	$\zeta = 0.26$	$\zeta = 0.11$	$\zeta = 0.14$	$\zeta = 0.13$	$\zeta = 0.20$	
State	Transition													
$^3B_1$	$b_1 \to 3sa_1$	6.30	5.95	6.56	6.29	6.93	7.54	6.80	7.39	7.16	7.32	7.06	7.46	7.00
$^1B_1$	$b_1 \to 3sa_1$	6.55	6.24	6.92	6.57	7.25	7.92	7.18	7.84	7.60	7.78	7.43	7.88	7.40
$^3A_2$	$b_1 \to 3pb_2$	7.59	7.25	8.19	7.50	8.58	9.43	8.50	9.28	8.99	9.19	8.66	9.21	8.90
$^1A_2$	$b_1 \to 3pb_2$	7.60	7.28	8.28	7.53	8.63	9.55	8.61	9.48	9.16	9.39	8.76	9.37	9.10
$^3A_1$	$a_1 \to 3sa_1$	8.27	7.97	8.60	8.34	8.92	9.55	8.83	9.43	9.22	9.38	9.12	9.52	9.30
$^1A_1$	$a_1 \to 3sa_1$	8.62	8.36	9.11	8.75	9.38	10.02	9.39	10.01	9.91	9.91	9.68	10.18	9.70
$^3A_1$	$b_1 \to 3pb_1$	7.98	7.60	8.58	7.83	9.00	10.02	8.98	9.99	9.58	9.85	9.04	9.70	9.81
$^3B_1$	$b_1 \to 3pa_1$	7.72	7.41	8.60	7.65	8.84	10.00	8.94	10.07	9.68	9.97	9.18	9.74	9.98
$^1B_1$	$b_1 \to 3pa_1$	7.75	7.44	8.62	7.69	8.86	10.02	8.96	10.10	9.70	9.99	9.22	9.77	10.01
$^1A_1$	$b_1 \to 3pb_1$	8.06	7.70	8.72	7.96	9.08	10.22	9.10	10.23	9.68	10.15	9.20	9.86	10.16
Mean absolute errors with respect to experiment														
Rydberg (10)		1.49	1.82	0.92	1.53	0.59	0.29	0.61	0.25	0.21	0.16	0.42	0.25	
All (10)		1.49	1.82	0.92	1.53	0.59	0.29	0.61	0.25	0.21	0.16	0.42	0.25	

[a]From Ref. [47].

Table 3.10: Valence and Rydberg excitation energies (in eV) for the N_2 molecule calculated by TDDFT using various density functionals with and without the correction by adding a fraction of nuclear charge ζ. Molecular geometry: $r(NN) = 1.098$Å.

| N_2 | | Uncorrected potentials | | | | Corrected potentials | | | | | | | | |
| | | $\zeta = 0$ | | | | $\zeta = 0.11$ | $\zeta = 0.22$ | $\zeta = 0.15$ | $\zeta = 0.26$ | $\zeta = 0.11$ | $\zeta = 0.14$ | $\zeta = 0.13$ | $\zeta = 0.20$ | |
State	Transition	LDA	BLYP	B3LYP	TPSS	LDA		BLYP		B3LYP		TPSS		Expt.[a]
$^3\Sigma_u^+$	$\pi_u \to \pi_g$	7.91	7.48	7.10	7.27	7.89	7.86	7.44	7.39	7.04	7.02	7.23	7.20	7.75
$^3\Pi_g$	$\sigma_g \to \pi_g$	7.58	7.45	7.58	7.46	7.60	7.61	7.47	7.47	7.59	7.59	7.48	7.48	8.04
$^3\Delta_u$	$\pi_u \to \pi_g$	8.84	8.22	7.97	8.10	8.86	8.86	8.21	8.20	7.94	7.93	8.09	8.07	8.88
$^1\Pi_g$	$\sigma_g \to \pi_g$	9.07	9.09	9.27	9.26	9.13	9.18	9.18	9.23	9.32	9.33	9.34	9.38	9.31
$^3\Sigma_u^-$	$\pi_u \to \pi_g$	9.68	9.58	9.33	9.88	9.72	9.75	9.64	9.67	9.35	9.35	9.93	9.95	9.67
$^1\Sigma_u^-$	$\pi_u \to \pi_g$	9.68	9.58	9.33	9.88	9.72	9.75	9.64	9.67	9.35	9.35	9.93	9.95	9.92
$^1\Delta_u$	$\pi_u \to \pi_g$	10.23	9.86	9.72	10.01	10.30	10.35	9.95	9.99	9.76	9.77	10.07	10.10	10.27
$^3\Pi_u$	$\sigma_u \to \pi_g$	10.38	10.32	10.64	10.64	10.50	10.61	10.50	10.61	10.77	10.80	10.81	10.89	11.19
$^3\Sigma_g^+$	$\sigma_g \to 3s\sigma_g$	10.42	10.06	11.02	10.39	11.27	12.12	11.21	12.05	11.85	12.08	11.41	11.97	12.00
$^1\Sigma_g^+$	$\sigma_g \to 3s\sigma_g$	10.61	10.26	11.29	10.60	11.49	12.37	11.45	12.34	12.16	12.40	11.66	12.24	12.20
$^1\Pi_u$	$\sigma_g \to 3p\pi_u$	10.94	10.60	11.71	10.95	11.89	12.86	11.90	12.87	12.66	12.92	12.10	12.72	12.9
$^1\Sigma_u^+$	$\sigma_g \to 3p\sigma_u$	10.83	10.50	11.69	10.84	11.84	12.85	11.87	12.89	12.66	12.93	12.05	12.71	12.98
$^1\Pi_u$	$\pi_u \to 3s\sigma_g$	11.97	11.37	12.06	11.73	12.83	13.73	12.55	13.41	12.90	13.13	12.78	13.33	13.24
$^1\Pi_u$	$\sigma_u \to \pi_g$	13.01	13.13	13.58	13.64	13.28	13.46	13.47	13.71	13.86	13.93	13.90	14.09	13.63
		Mean absolute errors with respect to experiment												
Valence (9)		0.29	0.44	0.46	0.33	0.23	0.20	0.35	0.32	0.46	0.47	0.34	0.36	
Rydberg (5)		1.71	2.11	1.11	1.76	0.80	0.19	0.87	0.10	0.22	0.09	0.66	0.12	
All (14)		0.80	1.03	0.69	0.84	0.44	0.19	0.54	0.24	0.37	0.33	0.45	0.28	

[a]From Ref. [48].

Bibliography

[1] E. Runge and E. K. U. Gross, "Density-functional theory for time-dependent systems", Phys. Rev. Lett. **52**, 997–1000 (1984).

[2] M. E. Casida, "Time-dependent density functional response theory for molecules", in *Recent Advances in Density Functional Methods* (World Scientific, Singapore, 1995), pp. 155–192.

[3] C. A. Ullrich, *Time-Dependent Density-Functional Theory: Concepts and Applications* (Oxford University Press, New York, 2012).

[4] R. Bauernschmitt and R. Ahlrichs, "Treatment of electronic excitations within the adiabatic approximation of time dependent density functional theory", Chem. Phys. Lett. **256**, 454–464 (1996).

[5] P. Elliott, F. Furche, and K. Burke, "Excited states from time-dependent density functional theory", in *Reviews in Computational Chemistry* (John Wiley & Sons, Inc., 2009), pp. 91–165.

[6] M. E. Casida and M. Huix-Rotllant, "Progress in time-dependent density-functional theory", Annu. Rev. Phys. Chem. **63**, 287–323 (2012).

[7] L. González, D. Escudero, and L. Serrano-Andrés, "Progress and challenges in the calculation of electronic excited states", ChemPhysChem **13**, 28–51 (2012).

[8] M. E. Casida, "Time-dependent density functional response theory of molecular systems: Theory, computational methods, and functionals", in *Recent Developments and Applications of Modern Density Functional Theory*, Vol. 4, edited by J. M. Seminario (Elsevier, 1996), pp. 391–439.

[9] M. Petersilka, U. J. Gossmann, and E. K. U. Gross, "Excitation energies from time-dependent density-functional theory", Phys. Rev. Lett. **76**, 1212–1215 (1996).

[10] M. E. Casida, C. Jamorski, K. C. Casida, and D. R. Salahub, "Molecular excitation energies to high-lying bound states from time-dependent density-functional response theory: Characterization and correction of the time-dependent local density approximation ionization threshold", J. Chem. Phys. **108**, 4439–4449 (1998).

[11] J. P. Perdew and A. Zunger, "Self-interaction correction to density-functional approximations for many-electron systems", Phys. Rev. B **23**, 5048–5079 (1981).

[12] M. Caricato, G. W. Trucks, M. J. Frisch, and K. B. Wiberg, "Electronic transition energies: A study of the performance of a large range of single reference density functional and wave function methods on valence and Rydberg states compared to experiment", J. Chem. Theory Comput. **6**, 370–383 (2010).

[13] M. Isegawa, R. Peverati, and D. G. Truhlar, "Performance of recent and high-performance approximate density functionals for time-dependent density functional theory calculations of valence and Rydberg electronic transition energies", J. Chem. Phys. **137**, 244104 (2012).

[14] S. S. Leang, F. Zahariev, and M. S. Gordon, "Benchmarking the performance of time-dependent density functional methods", J. Chem. Phys. **136**, 104101 (2012).

[15] R. van Leeuwen and E. J. Baerends, "Exchange-correlation potential with correct asymptotic behavior", Phys. Rev. A **49**, 2421–2431 (1994).

[16] D. J. Tozer and N. C. Handy, "Improving virtual Kohn-Sham orbitals and eigenvalues: Application to excitation energies and static polarizabilities", J. Chem. Phys. **109**, 10180–10189 (1998).

[17] P. R. T. Schipper, O. V. Gritsenko, S. J. A. van Gisbergen, and E. J. Baerends, "Molecular calculations of excitation energies and (hyper)polarizabilities with a statistical average of orbital model exchange-correlation potentials", J. Chem. Phys. **112**, 1344–1352 (2000).

[18] M. Grüning, O. V. Gritsenko, S. J. A. van Gisbergen, and E. J. Baerends, "Shape corrections to exchange-correlation potentials by gradient-regulated seamless connection of model potentials for inner and outer region", J. Chem. Phys. **114**, 652–660 (2001).

[19] R. van Meer, O. V. Gritsenko, and E. J. Baerends, "Physical meaning of virtual Kohn-Sham orbitals and orbital energies: An ideal basis for the description of molecular excitations", J. Chem. Theory Comput. **10**, 4432–4441 (2014).

[20] A. D. Becke and E. R. Johnson, "A simple effective potential for exchange", J. Chem. Phys. **124**, 221101 (2006).

[21] A. Karolewski, R. Armiento, and S. Kümmel, "Electronic excitations and the Becke-Johnson potential: The need for and the problem of transforming model potentials to functional derivatives", Phys. Rev. A **88**, 052519 (2013).

[22] Y. Zhao, and D. G. Truhlar, "Density functional for spectroscopy: No long-range self-interaction error, good performance for Rydberg and charge-transfer states, and better performance on average than B3LYP for ground states", J. Phys. Chem. A **110**, 13126–13130 (2006).

[23] H. Iikura, T. Tsuneda, T. Yanai, and K. Hirao, "A long-range correction scheme for generalized-gradient-approximation exchange functionals", J. Chem. Phys. **115**, 3540–3544 (2001).

[24] T. Yanai, D. P. Tew, and N. C. Handy, "A new hybrid exchange-correlation functional using the Coulomb-attenuating method (CAM-B3LYP)", Chem. Phys. Lett. **393**, 51–57 (2004).

[25] O. A. Vydrov and G. E. Scuseria, "Assessment of a long-range corrected hybrid functional", J. Chem. Phys. **125**, 234109 (2006).

[26] J.-D. Chai and M. Head-Gordon, "Long-range corrected hybrid density functionals with damped atom-atom dispersion corrections", Phys. Chem. Chem. Phys. **10**, 6615–6620 (2008).

[27] A. P. Gaiduk, D. S. Firaha, and V. N. Staroverov, "Improved electronic excitation energies from shape-corrected semilocal Kohn-Sham potentials", Phys. Rev. Lett. **108**, 253005 (2012).

[28] A. P. Gaiduk, D. Mizzi, and V. N. Staroverov, "Self-interaction correction scheme for approximate Kohn-Sham potentials", Phys. Rev. A **86**, 052518 (2012).

[29] C. J. Umrigar, A. Savin, and X. Gonze, "Are unoccupied Kohn-Sham eigenvalues related to excitation energies?", in *Electronic Density Functional Theory: Recent Progress and New Directions*, edited by J. F. Dobson, G. Vignale, and M. P. Das (Springer US, Boston, MA, 1998), pp. 167–176.

[30] S. L. Li and D. G. Truhlar, "Testing time-dependent density functional theory with depopulated molecular orbitals for predicting electronic excitation energies of valence, Rydberg, and charge-transfer states and potential energies near a conical intersection", J. Chem. Phys. **141**, 104106 (2014).

[31] A. D. Becke, "Density-functional thermochemistry. III. The role of exact exchange", J. Chem. Phys. **98**, 5648–5652 (1993).

[32] C. Lee, W. Yang, and R. G. Parr, "Development of the Colle-Salvetti correlation-energy formula into a functional of the electron density", Phys. Rev. B **37**, 785–789 (1988).

[33] A. D. Becke, "Density-functional exchange-energy approximation with correct asymptotic behavior", Phys. Rev. A **38**, 3098–3100 (1988).

[34] Y. Zhao and D. G. Truhlar, "The M06 suite of density functionals for main group thermochemistry, thermochemical kinetics, noncovalent interactions, excited states, and transition elements: Two new functionals and systematic testing of four M06-class functionals and 12 other functionals", Theor. Chem. Acc. **120**, 215–241 (2008).

[35] J. F. Stanton and R. J. Bartlett, "The equation of motion coupled-cluster method. A systematic biorthogonal approach to molecular excitation energies, transition probabilities, and excited state properties", J. Chem. Phys. **98**, 7029–7039 (1993).

[36] W. Kohn and L. J. Sham, "Self-consistent equations including exchange and correlation effects", Phys. Rev. **140**, A1133–A1138 (1965).

[37] M. J. Frisch, G. W. Trucks, H. B. Schlegel, G. E. Scuseria, M. A. Robb, J. R. Cheeseman, G. Scalmani, V. Barone, B. Mennucci, G. A. Petersson, H. Nakatsuji, M. Caricato, X. Li, H. P. Hratchian, A. F. Izmaylov, J. Bloino, G. Zheng, J. L. Sonnenberg, M. Hada, M. Ehara, K. Toyota, R. Fukuda, J. Hasegawa, M. Ishida, T. Nakajima, Y. Honda, O. Kitao, H. Nakai, T. Vreven, J. A. Montgomery Jr., J. E. Peralta, F. Ogliaro, M. Bearpark, J. J. Heyd, E. Brothers, K. N. Kudin, V. N. Staroverov, R. Kobayashi, J. Normand, K. Raghavachari, A. Rendell, J. C. Burant, S. S. Iyengar, J. Tomasi, M. Cossi, N. Rega, J. M. Millam, M. Klene, J. E. Knox, J. B. Cross, V. Bakken, C. Adamo, J. Jaramillo, R. Gomperts, R. E. Stratmann, O. Yazyev, A. J. Austin, R. Cammi, C. Pomelli, J. W. Ochterski, R. L. Martin, K. Morokuma, V. G. Zakrzewski, G. A. Voth, P. Salvador, J. J. Dannenberg, S. Dapprich, A. D. Daniels,. Farkas, J. B. Foresman, J. V. Ortiz, J. Cioslowski, and D. J. Fox, *Gaussian 09, Revision D.01*, Gaussian Inc., Wallingford, CT, 2009.

[38] A. Savin, C. Umrigar, and X. Gonze, "Relationship of Kohn-Sham eigenvalues to excitation energies", Chem. Phys. Lett. **288**, 391–395 (1998).

[39] J. P. Perdew and Y. Wang, "Accurate and simple analytic representation of the electron-gas correlation energy", Phys. Rev. B **45**, 13244–13249 (1992).

[40] J. Tao, J. P. Perdew, V. N. Staroverov, and G. E. Scuseria, "Climbing the density functional ladder: Nonempirical meta-generalized gradient approximation designed for molecules and solids", Phys. Rev. Lett. **91**, 146401 (2003).

[41] A. Kramida, Y. Ralchenko, and J. Reader, *NIST Atomic Spectra Database* (version 5.3), edited by National Institute of Standards and Technology, Gaithersburg, MD.

[42] E. S. Nielsen, P. Jörgensen, and J. Oddershede, "Transition moments and dynamic polarizabilities in a second order polarization propagator approach", J. Chem. Phys. **73**, 6238–6246 (1980).

[43] D. J. Clouthier and D. A. Ramsay, "The spectroscopy of formaldehyde and thioformaldehyde", Annu. Rev. Phys. Chem. **34**, 31–58 (1983).

[44] R. Dressler and M. Allan, "A dissociative electron attachment, electron transmission, and electron energyloss study of the temporary negative ion of acetylene", J. Chem. Phys. **87**, 4510–4518 (1987).

[45] A. S. Zyubin and A. M. Mebel, "Accurate prediction of excitation energies to highlying Rydberg electronic states: Rydberg states of acetylene as a case study", J. Chem. Phys. **119**, 6581–6587 (2003).

[46] L. Serrano-Andrés, M. Merchán, I. Nebot-Gil, R. Lindh, and B. O. Roos, "Towards an accurate molecular orbital theory for excited states: Ethene, butadiene, and hexatriene", J. Chem. Phys. **98**, 3151–3162 (1993).

[47] A. Chutjian, R. I. Hall, and S. Trajmar, "Electron-impact excitation of H_2O and D_2O at various scattering angles and impact energies in the energy-loss range 4.2–12 eV", J. Chem. Phys. **63**, 892–898 (1975).

[48] S. B. Ben-Shlomo and U. Kaldor, "N_2 excitations below 15 eV by the multireference coupled-cluster method", J. Chem. Phys. **92**, 3680–3682 (1990).

Chapter 4

Summary

Density functional approximations enjoy great popularity in applied quantum chemistry due to their low computational cost in combination with decent accuracy. Despite this success, there exist obstacles that prevent DFAs from being used as a universal black-box tool to calculate any properties of any system. The lack of derivative discontinuity [1], which is also reflected in the incorrect asymptotic shape of the exchange-correlation potential, causes complications with a number of properties, such as incorrect energies of the highest occupied and the lowest unoccupied molecular orbital, unphysical charges on dissociating fragments [2, 3], and inaccurate Rydberg excitation energies [4, 5].

In an attempt to design corrections that address the consequences of the lack of derivative discontinuity, one has to take certain desirable features into account. First of all, the correction scheme should preserve the already satisfactory accuracy of DFAs for the majority of properties. Second, the correction should not increase the running time of a density functional calculation significantly, otherwise, one of the main advantages of DFT, its low computational cost, will be lost. Finally, it would be preferable if the correction scheme had as little system dependence as possible. The method of fractional population of frontier molecular orbitals aims to satisfy these criteria. In this method, the shape-corrected exchange-correlation potential is generated on the fly from the exchange-correlation potential of the fractionally depopulated or fractionally populated system.

In Chapter 1 of the present work, we showed that, in addition to the improved orbital eigenvalues and vertical excitation energies [6, 7], the method of fractional occupations solves the problem of fractional charges on atoms in dissociating molecules. We designed an algorithm to decide which orbital is to be fractionally occupied and what its occupation number should be. By means of this algorithm, it is possible to model the step structure of the exact exchange-correlation potential in polar diatomic molecules. We demonstrated that our scheme provides qualitatively correct behavior of charges as the distance between

the dissociating atoms increases.

A fractionally charged system can be also created by modifying the nuclear charges of the atoms in a molecule. In Chapter 2, we employed this approach to obtain corrected exchange-correlation potentials to be used in time-dependent DFT calculations. Although addition of nuclear charge did lead to some improvements in Rydberg excitation energies, the amount of charge to be added appeared to be system-dependent. This showed that it is not only the sheer presence of fractional charge, but also its distribution that plays a role in correcting the shape of the exchange-correlation potential and related properties.

Bibliography

[1] J. P. Perdew, "Size-consistency, self-interaction correction, and derivative discontinuity in density functional theory", in *Density Functional Theory of Many-Fermion Systems*, edited by P.-O. Löwdin (Academic Press, 1990), pp. 113 –134.

[2] J. P. Perdew, R. G. Parr, M. Levy, and J. L. Balduz, "Density-functional theory for fractional particle number: Derivative discontinuities of the energy", Phys. Rev. Lett. **49**, 1691–1694 (1982).

[3] A. Ruzsinszky, J. P. Perdew, G. I. Csonka, O. A. Vydrov, and G. E. Scuseria, "Spurious fractional charge on dissociated atoms: Pervasive and resilient self-interaction error of common density functionals", J. Chem. Phys. **125**, 194112 (2006).

[4] M. Petersilka, U. J. Gossmann, and E. K. U. Gross, "Excitation energies from time-dependent density-functional theory", Phys. Rev. Lett. **76**, 1212–1215 (1996).

[5] M. E. Casida, C. Jamorski, K. C. Casida, and D. R. Salahub, "Molecular excitation energies to high-lying bound states from time-dependent density-functional response theory: Characterization and correction of the time-dependent local density approximation ionization threshold", J. Chem. Phys. **108**, 4439–4449 (1998).

[6] A. P. Gaiduk, D. S. Firaha, and V. N. Staroverov, "Improved electronic excitation energies from shape-corrected semilocal Kohn-Sham potentials", Phys. Rev. Lett. **108**, 253005 (2012).

[7] A. P. Gaiduk, D. Mizzi, and V. N. Staroverov, "Self-interaction correction scheme for approximate Kohn-Sham potentials", Phys. Rev. A **86**, 052518 (2012).

Appendix A

On the shape of the PBE exchange potential in interatomic regions

In order to exclude any possible numerical artefacts and simplify the problem, an analytical function was chosen to model the one-dimensional density in the region between two nuclei. We make use of the fact that atomic densities are approximately piecewise exponential [1]. Thus, two identical atoms that are well separated from each other can be modeled by the sum of two exponents:

$$\rho = e^{-(x+r/2)} + e^{(x-r/2)}, \tag{A.1}$$

where by tuning the parameter r one can simulate an increasing interatomic separation.

To reconstruct the PBE exchange potential, one needs four ingredients: the density ρ, the dimensionless density gradient s, Laplacian q, and Hessian u [2]:

$$s = \frac{|\nabla\rho|}{\rho^{4/3}}, \tag{A.2}$$

$$q = \frac{\nabla^2\rho}{\rho^{5/3}}, \tag{A.3}$$

$$u = \frac{(\nabla\rho)^2\nabla|\nabla\rho|}{\rho^{13/3}}. \tag{A.4}$$

It is clear from Fig. A.1, that in the region between two sufficiently separated nuclei, where the density is nearly flat, all the three dimensionless ingredients are ill behaved.

The PBE exchange energy functional has the general form

$$E[\rho] = \int f(\rho, s)d\mathbf{r}, \tag{A.5}$$

where f is the energy-density function for the PBE functional [3],

$$f(\rho, s) = C\rho^{4/3}\left(1 + \frac{\mu s^2}{1 + \frac{\mu s^2}{k}}\right).$$

(A.6)

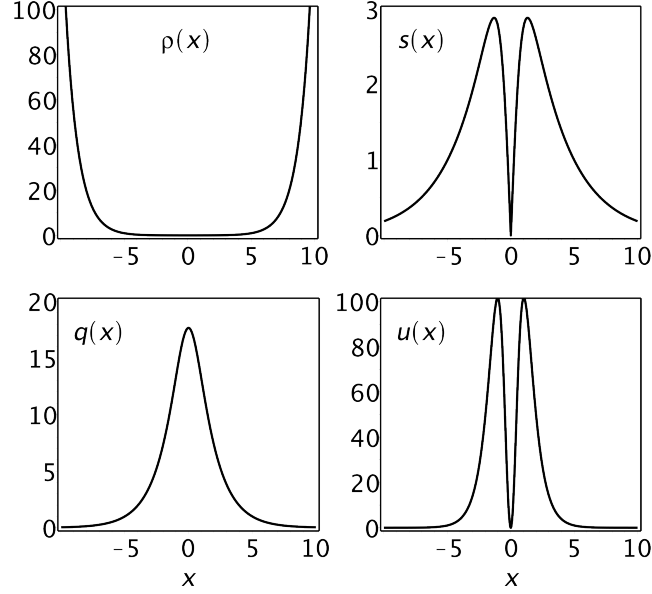Here C, μ, and k are non-empirical parameters.

Figure A.1: The four ingredient of the PBE exchange potential for the model one-dimensional exponential density of Eq. A.1.
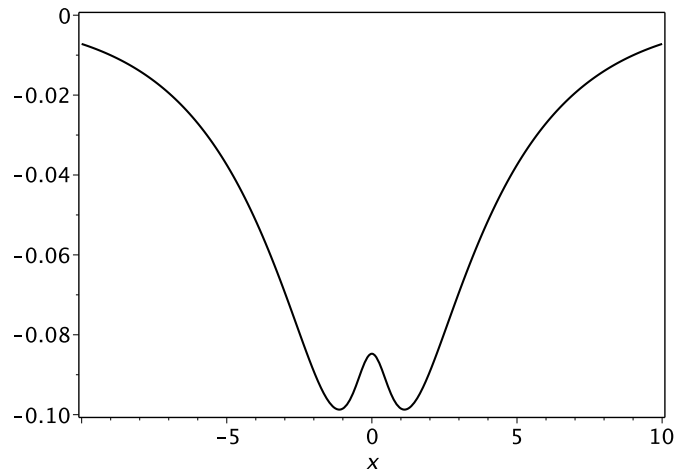

Figure A.2: The sum of the last five components of Eq. A.7 for the PBE exchange potential evaluated using model one-dimensional exponential density. These components are the source of the spikes in v_X^{PBE}.

The exchange potential was constructed according to Ref. [2] as the sum of the following six terms:

$$
\begin{aligned}
v_X =& \frac{\partial f}{\partial \rho} + \frac{4}{3} \frac{\partial^2 f}{\partial s^2} \frac{s^2}{\rho} - \frac{\partial^2 f}{\partial \rho \partial s} s - \frac{\partial f}{\partial s} \frac{q}{\rho s} \\
& + \frac{\partial f}{\partial s} \frac{u}{\rho s^3} - \frac{\partial^2 f}{\partial s^2} \frac{u}{\rho s^2}.
\end{aligned}
\tag{A.7}
$$

Substituting the one-dimensional model density and the three corresponding dimensionless components into Eq. A.7 results in five of the six terms having minima at $x = 0$, and two of them (the second and the third) also having inflection points near $x = 0$. When these five terms are summed up, the irregularities do not cancel out (Fig. A.2). In calculations on real systems, the problem may be further enhanced by numerical artefacts, but it does not affect neither energies, nor molecular properties.

Bibliography

[1] W.-P. Wang and R. G. Parr, "Statistical atomic models with piecewise exponentially decaying electron densities", Phys. Rev. A **16**, 891–902 (1977).

[2] A. P. Gaiduk and V. N. Staroverov, "Construction of integrable model Kohn-Sham potentials by analysis of the structure of functional derivatives", Phys. Rev. A **83**, 012509 (2011).

[3] J. P. Perdew, K. Burke, and M. Ernzerhof, "Generalized gradient approximation made simple", Phys. Rev. Lett. **77**, Errata: **78**, 1396(E) (1997), 3865–3868 (1996).

Curriculum Vitae

Name: Darya N. Komsa

Post-Secondary   M.Sc. in Chemistry (2014–2016)
Education and   University of Western Ontario, London, ON
Degrees: Advisor: Professor Viktor N. Staroverov

                       B.Sc. in Chemistry (2009–2014)
                       Belarusian State University, Minsk, Belarus
                       Advisor: Dr. Vitaly E. Matulis

Honours and   Christian Sivertz Scholarship (2014)
Awards:
                       3d Prize, Belarusian Chemistry Olympiad
                       for University Students (2010)

                       1st Prize, Belarusian National High-School
                       Chemistry Olympiad (2009)

Related Work   Graduate Teaching Assistant (2014–2016)
Experience: The University of Western Ontario
                       – Computer Methods in Chemistry (Winter 2015, 2016)
                       – Physical Chemistry for Life Sciences (Winter 2016)
                       – Discovering Chemical Structure (Fall 2014, 2015)

                       eLearning content developer (2012–2015)
                       Competentum Group, Inc., Minsk, Belarus

                       Visiting Undergraduate Student (2013)
                       The University of Western Ontario
                       Supervisor: Professor Viktor N. Staroverov

Publications:

3. **D. N. Komsa** and V. N. Staroverov, "Do fractional nuclear charges improve calculated Rydberg excitation energies as reliably as HOMO depopulation?", manuscript in preparation.

2. **D. N. Komsa** and V. N. Staroverov, "Elimination of spurious fractional charges in dissociating molecules by correcting the shape of approximate Kohn-Sham potentials", J. Chem. Theory Comput., submitted manuscript.

1. M. N. Nichick, S. V. Voiteckhovich, V. E. Matulis, **D. N. Komsa**, A. I. Lesnikovich, and O. A. Ivashkevich, "5-Mercaptotetrazole-1-acetic acid as a novel caping ligand for stabilization of metal nanoparticles in water", in *Physics, Chemistry and Application of Nanostructures: Proceedings of International Conference Nanomeeting – 2013* (World Scientific Publishing, 2013), pp. 282–286.

Conference Presentations:

"Elimination of spurious fractional charges in dissociating molecules by correcting the shape of approximate Kohn-Sham potentials", 2015 Symposium on Chemical Physics, The University of Waterloo, Waterloo, Ontario, November 6–8, 2015 (talk).